NANOG MODIFICATION AND DEGRADATION IN MURINE EMBRYONIC STEM CELLS

by

HOPE E. BLACKSTONE

(Under the Direction of Stephen Dalton and J. David Puett)

ABSTRACT

Embryonic stem cells are pluripotent progenitors for virtually all cell types in our body and contain limitless potential for therapeutic use and regenerative medicine. Murine embryonic stem cells can be maintained as a self-renewing, pluripotent population by LIF/STAT3-dependent signaling, and are regulated by a combination of extrinsic and intrinsic factors. The nuclear transcription factor, Nanog, plays a key role in maintaining these stem cell properties. However, little is known about the regulation of Nanog or its degradation during differentiation. This research is focused on elucidating the possible relationship between Nanog and other factors that could play a role in Nanog degradation.

INDEX WORDS: Embryonic Stem Cells, Nanog, Self-renewal, Pluripotency

# NANOG MODIFICATION AND DEGRADATION IN MURINE EMBRYONIC STEM CELLS

by

HOPE BLACKSTONE

B.S., University of Maine, 2005

A Thesis Submitted to the Graduate Faculty of The University of Georgia in Partial Fulfillment of the Requirements for the Degree

MASTER OF SCIENCE

ATHENS, GEORGIA

2008

# NANOG MODIFICATION AND DEGRADATION IN MURINE EMBRYONIC STEM CELLS

by

HOPE E. BLACKSTONE

| | |
|---|---|
| Major Professors: | Stephen Dalton<br>J. Dave Puett |
| Committee: | Michael Tiemeyer<br>Scott Dougan |

Electronic Version Approved:

Maureen Grasso
Dean of the Graduate School
The University of Georgia
August 2008

# DEDICATION

For my incredible family, who offered me unconditional (long distance) love and support throughout the course of this thesis. For my irreplaceable friends, who have been like family to me, and I am truly thankful for. For my grandfather, whose love for life and others will be the example that I will live my life trying to emulate, and who I know would be 'Big Proud'.

Philippians 4:13

ACKNOWLEDGEMENTS

I would like to that thank my supervisors, Dr. Dalton and Dr. Puett, for their guidance and support in my pursuit of my Master's degree here at the University of Georgia. I also would like to thank all of labmates from both the Dalton and Puett labs for all of their advice and assistance through out the duration of this project. Also, a very special thank-you to two of my labmates, Geneva DeMars and Keriayn Smith, for their daily kindness and encouragement, which was truly a blessing.

TABLE OF CONTENTS

Page

**LIST OF FIGURES** Page

# Chapter 1. Introduction

## 1.1. Early Embryonic Development and Embryonic Stem Cells

### 1.1.1. Background

Mammalian embryogenesis is the process by which a single fertilized egg undergoes a complex series of tightly regulated events to give rise to all three germ layers, creating organs and structures of the mature organism. Embryogenesis can be broken down into distinct stages in which different levels of development occur. In the early mammalian embryo, in a stage known as the blastocyst, there exists a transient dynamically regulated population of pluripotent cells located in the inner cell mass (ICM). This population of cells gives rise to Embryonic Stem Cells (ESC) when they are plated in culture. These cells have the potential to differentiate and contribute to the three primary germ layers: endoderm, ectoderm, and mesoderm. These cells are also defined by their ability to self-renew and maintain their pluripotent state. Self-renewal is defined as the ability to go through numerous cycles of cell division while maintaining the undifferentiated state, and pluripotency is the capacity to differentiate into specialized cell types from any of the three germ layers. Much attention has recently been directed towards understanding the signals, and the mechanisms of these signals which regulate ESC differentiation events, for its implications in possible therapeutic applications. The identification and mechanism of these interactions that influence pluripotent ESC is the major focus of this thesis.

### 1.1.2. Early Embryonic Development

As previously described, embryogenesis is the process by which a fertilized egg undergoes a series of divisions to give rise to cells of all three germ layers; these include

more than 220 cell types in the adult body. Early embryonic development involves a tightly regulated and complex pattern of events from zygote, i.e. a fertilized egg. The zygote undergoes rapid mitotic divisions; two exact genetic replicates of the original cell are formed, with no significant growth (a process known as cleavage). Numerous rounds of cellular division produce a cluster of cells the same size as the original zygote, at this stage the cells are a morula (Fig. 1). It is at this stage that the interior cells form the inner cell mass, and the outer layer will give rise to the trophoblast. Cells of the ICM are pluripotent and will give rise to the embryo proper, while the trophoblast cells will differentiate into the placenta and other supporting tissues (Johnson and Ziomek 1981). When the embryo is comprised of approximately 120 cells, it is referred to as a blastula; ESCs are removed from the ICM component of the blastocyst. ICM cells adjacent to the blastocoel begin to differentiate into a second extra-embryonic epithelial layer, known as the primitive endoderm (Watson and Kidder 1988). The primitive endoderm then goes on to give rise to the visceral endoderm, which remains in contact with the embryo until gastrulation when it is displaced and forms the visceral yolk sac (Gardner 1983). The primitive endoderm that contacts the trophoectoderm migrates laterally to the blastocoel and forms the parietal endoderm (Gardner, 1983). Implantation of the embryo into the uterine wall then occurs alongside the formation of the proamniotic cavity within the ICM. The ICM begins to organize as an epithelial sheet, called the primitive ectoderm, and in conjunction with the embryo proper, is now defined as an epiblast (Coucouvanis and Martin 1995).

### 1.1.3. Embryonic Stem Cell Derivation

Embryonic Stem Cells are derived from the ICM of pre-implantation blastocyst

stage embryo (Fig.1) (Rasmussen 2003). ESCs retain their pluripotent characteristics when cultured under the appropriate conditions, and can be re-injected into the blastocyst where they have the capacity to generate all somatic and germ cell lineages. ESCs can either be cultured as a monolayer grown on MEFs (mouse embryonic fibroblasts) or in suspension as embryoid bodies (EBs). EBs can be a useful model when looking at spontaneous differentiation. The differentiation patter of EBs mimics that of a developing embryo *in vivo*, with exceptions, including the lack of the spatial organization. However, the temporal order and formation of the primitive endoderm, primitive ectoderm, and further differentiated derivatives closely match those of the developing ICM *in vivo* (Beddington and Robertson 1989).

### 1.1.4. Embryonic Stem Cell Maintenance and Pluripotency

As previously stated, ESC can be maintained *in vitro* by defined culture conditions. Currently, ESC research is heavily focused on two mammalian models; human ESCs (hESCs) and murine ESCs (mESCs). Although, there are many similarities in their derivation and maintenance there are also critical differences. mESCs are maintained in their pluripotent state through a signal transduction pathway that requires the gp130 receptor, the interleukin-6 (IL-6) family of cytokines, and the Janus Kinase signal transducer and activator (JAK/STAT) pathway (Fig. 2) (Humphrey, Beattie et al. 2004). mESCs had historically been maintained in culture on a feeder layer of mitotically inactivated mouse embryonic feeders (MEFs), it was later discovered that the mESCs could be maintained on gelatin in MEF conditioned media, eliminating the need for a feeder layer. It was then subsequently demonstrated that MEFs inhibit ESC differentiation through their production of the IL-6 family cytokine, Leukemia Inhibitory

Factor (LIF) (s. Yamanaka 2006; Yamanaka 2006). Addition of LIF in the absence of MEFs in defined mESC media is sufficient to activate the STAT3 pathway and block mESC differentiation and maintain mESC characteristics; however, it is insufficient to prevent differentiation in hESC, and has been demonstrated that STAT3 activation alone is unable to maintain hESC (Humphrey, Beattie et al. 2004). This indicates key differences in the signals necessary to maintain human and mouse ESCs. This thesis is focused on mESCs and the factors that have an effect on their pluripotency and maintenance.

## 1.2. Mouse Embryonic Stem Cell Self Renewal and Pluripotency

### 1.2.1. STAT3 signaling and LIF

Signal Transducers and Activators of Transcription (STATs), are transcription factors that are phosphorylated by JAK kinases in response to cytokine activation of a cell surface receptor tyrosine kinase. Upon activation, the STATs dimerize and are localized to the nucleus where they activate transcription of cytokine-responsive genes (Hideaki Nakajima 2001; Nakajima 2001). Leukemia Inhibitory Factory (LIF) is the established self-renewal factor for mESCs. LIF is a cytokine belonging to the interleukin (IL)-6-type family, which signal through the common receptor subunit gp130, along with the ligand specific subunit, such as the LIF receptor LIFR$\beta$. This binding results in the activation on the canonical Jak pathway, resulting in Jak kinase phosphorylating tyrosine residues on both gp130 and LIFR$\beta$. This specific phosphorylation recruits STAT1 and STAT3 through their SH2 domains. These Stat proteins are then activated by Jak-mediated tyrosine phosphorylation to form homodimers and/or heterodimers and translocate to the nucleus, where they function as transcription factors (Auernhammer

and Melmed 2000). It has been previously reported that STAT3 activation is essential and sufficient to maintain the self-renewal and pluripotential of mouse ESCs (Niwa, Burdon et al. 1998); (T Matsuda 1999). When STAT3 signaling is inactive *in vitro* mESCs spontaneously differentiate into a morphologically mixed population of cells, expressing genes characteristic of endoderm and mesoderm (Niwa, Burdon et al. 1998).

Many downstream effectors of this pathway are yet to be defined, but one important contributor is the protein c-Myc. c-myc is a protooncogene that encodes for a transcription factor that regulates expression of approximately 15% of all genes through binding on Enhancer Box sequences (E-boxes) and recruiting histone acetyltransferases (HATs) (Lüscher 2001). c-Myc belongs to the Myc family of transcription factors, which also includes N-Myc and L-Myc genes. Myc-family transcription factors contain the βHLH/LZ (basic Helix-Loop-Helix Leucine Zipper) domain (Lüscher 2001). Protein levels of Myc are high in pluripotent mESCs. Upon removal of LIF, Myc mRNA levels decrease and Myc protein is degraded. This degradation has been shown to be dependent on GSK3$\beta$ phosphorylation (Cartwright, McLean et al. 2005).

### 1.2.2. Intracellular Signaling Pathways Involved in ESC Maintenance

The complexity of the networks and signals that are responsible for mESC maintenance is immense, and is currently an extensively studied topic. Here, I will discuss the main transcriptional pathways responsible for stem cell maintenance and their interactions and cross talk between one another. These extrinsic pathways regulate intrinsic signals responsible for mESC regulation. As previously described, the STAT3/gp130/LIF signaling pathway is largely responsible for maintaining mESC in their pluripotent and self renewing state. However, this is only the beginning of

understanding the extensive interactive network responsible for stem cell maintenance. Cooperation and balance between multiple interacting pathways are necessary for proper maintenance of mESCs.

#### 1.2.2.1 BMP/Smad Pathway

Along with Stat3 activation by LIF, the BMP/Smad pathway has also been shown to suppress differentiation *in vivo*. Bone Morphogenic Proteins (BMP) are members of the transforming growth factor $\beta$ (TGF-$\beta$) superfamily. BMPs are secreted ligands that bind to type II receptor tyrosine kinases (BMPRII) (Koinuma 2003). This binding initiates the formation of the receptor components and causes the phosphorylation of Smads. Smads are intracellular transduction molecules that fall into three categories: receptor-regulated Smads (R-Smads), cooperating Smads (C-Smads), and inhibitory Smads (I-Smads). Upon BMP binding and activation, R-Smads (Smad1, Smad5 and Smad8) are phosphorylated at two C-terminal serine residues and form heterotrimeric complexes with Smad4. The Smad complexes are then able to translocate to the nucleus and function as transcription factors to block differentiation, primarily neuronal differentiation (Daizo Koinuma 2003). As previously stated, LIF addition is sufficient to maintain mESC in defined media containing serum. However, upon removal of serum, LIF was no longer able to prevent differentiation. Addition of BMP4 and LIF cooperatively maintained mESC in serum-free culture conditions(Ying 2002). In contrast, addition of BMP4 alone facilitated mesodermal differentiation of mESCs. This data suggests that the self-renewal and pluripotency of mESCs is achieved by a delicate balance between the two cytokines, LIF and BMP (Yamanaka 2006).

#### 1.2.2.2 Ras/ERK pathway

Another pathway that coordinately regulates mESC status is the Ras/ERK pathway. The protein Ras belongs to a superfamily of low molecular weight GTP-binding proteins that controls cell proliferation and differentiation in a variety of cells. Many different growth factors are known to be activators of Ras signaling by binding to receptor tyrosine kinases. This leads to the autophosphorylation of tyrosine residues on the receptors, which causes activation and ultimate binding to many downstream effector proteins including one called Raf. Raf is a serine/threonine kinase which then activates extracellular signal-regulated kinase (ERK). This pathway leads to activation of transcription factors, and ultimately suppresses self-renewal and promotes differentiation (J T Lee Jr 2002; Lee 2002). Therefore, ERK must be inhibited to support self-renewal and pluripotency. ERK can be inhibited by activated AKT, also known as protein kinase B, which can be achieved by activation of the Phosphatidyl Inositol 3 (PI3) Kinase Pathway (Yoshida-Koide, Matsuda et al. 2004).

#### 1.2.2.3. Phosphatidyl Inositol 3 Kinase Pathway

PI3 kinases are lipid kinases that catalyze the phosphorylation of inositol phospholipids at the third carbon position of the inositol ring (Cantley 2002). PI3 kinases are divided into three major classes (Class I, II, and III) based on substrate specificity, amino acid sequence, and the homology of its lipid kinase domain. Activation on the 1A PI3 kinases is induced by many different receptor tyrosine kinases for growth factors, including, fibroblast growth factor, epidermal growth factor, and platelet-derived growth factor. These activations lead to the generation of the second messenger

phosphatidylinositol 3,4,5-tris-phosphate ($PIP_3$). $PIP_3$ has a pleckstrin homology (PH) domain which allows binding to a serine/threonine kinase, AKT1. This complex is then translocated to the inner cell membrane, where it is phosphorylated and activated by PDK1, another serine/threonine kinase. Activated AKT1 is able to modulate the function of numerous substrates important in ESC maintenance (Cantley 2002). Recently the PI3K pathway has been shown to contribute to the maintenance of mESC pluripotency. The PI3K pathway regulates both directly and indirectly many proteins important for mESC. Treatment of mESCs with PI3K inhibitor, LY294002, suppressed progression of cell cycle and decreased cell proliferation (Ludmila Jirmanova 2002) playing a functional role in loss of pluripotency. A caveat to this is that PI3K signaling also leads to an inactivation of GSK3$\beta$, and inactivation of GSK3$\beta$ promotes pluripotency (Storm, Bone et al. 2007). This interaction is not yet fully understood, and like many other pathways involved in stem cell regulation, it seems that the relationship between PI3K signaling and GSK3$\beta$ inactivation may be involved in a larger transcriptional network.

#### 1.2.2.4 The Wnt/β-Catenin Pathway

The Wnt/$\beta$-Catenin pathway has been shown to have an effect on proliferation and differentiation, but its precise role remains somewhat elusive. The canonical Wnt pathway is dependent on the availability of a cytoplasmic protein, $\beta$-catenin. $\beta$-catenin functions in cell adhesion by linking cadherins to the actin cytoskeleton, and also as an intracellular signaling molecule (Reya and Clevers 2005). In the absence of Wnt activation, $\beta$-Catenin is phosphorylated by the adenomatous polyposis coli gene (APC), Axin, and glycogen synthase kinase (GSK) 3$\beta$ complex. Phosphorylated $\beta$-Catenin is marked for degradation by ubiquitin and sent to the proteasome, thus keeping the levels

of cytoplasmic $\beta$-Catenin low. However, when Wnt binds to its receptors, Frizzled and LRP5/6, GSK3$\beta$ is inactivated and lost from the complex, leaving $\beta$-Catenin unphosphorylated. This allows for cytoplasmic accumulation of $\beta$-Catenin , which is followed by its translocation into the nucleus where it associates with lymphoid enhancer factor (LEF)/T-cell factor (TCF) transcription factors (Yamanaka 2006). Wnt signaling has been shown to be important in neural differentiation of mESC, by overexpression of Wnt1, or by inhibition of GSK3$\beta$ (Aubert, Dunstan et al. 2002). Additionally, Wnt3a mutant mice display ectopic neural tube formation in the primitive streak of the gastrulating embryo (Yoshikawa, Fujimori et al. 1997) and, ESC with a mutated form of APC have an impaired ability to differentiate and contribute to all the germ layers (Kielman, Rindapaa et al. 2002). These findings conclude that Wnt signaling may suppress differentiation in ESC. (Sato, Meijer et al. 2004)

### 1.2.3. Murine Embryonic Stem Cell Epigenetic Regulation

Maintenance of ESCs is not only regulated by signal transduction pathways and gene transcription, but also by the accessibility of these signals to reach their target. The genome of stem cells is largely euchromatic, and areas are selectively silenced into heterochromatin along differentiation pathways (Jackson 2004). A series of recent studies have shown that mouse and human ESC possess epigenetic features, called Polycomb-group (PcG) complex proteins, which act to stabilize a repressive chromatin structure (Calrone 2005). Polycomb repressive complex 2 (PRC2), consisting of Ezh2, Eed and Suz12 in ES cells, acts as a histone methyltransferase on lysine 27 (K27) of histone H3. This results in its tri-methylation (H3K27me3), this is a trademark of transcriptionally inactive genes (Zhang, Cao et al. 2004). Intuitively, the appearance of

this silencing methylation is separate from the activating methylation on histone H3 of lysine 4 (H3K4me3) (Rea, Eisenhaber et al. 2000). However, it has been reported that these opposing histone methylation marks co-localize in particular regions of mouse ESC, called 'bivalent regions' (Bernstein, Mikkelsen et al. 2006). By genome wide ChIP on Chip analysis, over half of these bivalent domains that have been mapped have been shown to contain target sites that are common to genes that are heavily relied upon to maintain the ESC state (Oct3/4, Sox2, and Nanog) (Orkin 2005). These results suggest that, these bivalent domains could be markers for areas in the genome that are 'differentiation-ready', as proposed by the model from Szutoristz and Dillon. They propose that most tissue specific genes in ES cells would be targets for sequence specific factors that can recruit histone-modifying enzymes, resulting in the formation of 'early transcription competence marks' (ETCMs). ETCM are enriched for histone H3 and H4 acetylation, and H3K4me3, all of which are associated with transcriptionally active regions (Henrietta Szutorisz 2005; Szutorisz 2005). In both bivalent domains and ETCMs, H3K4me3 (active) marks spread as the genes near them become transcriptionally active, whereas H3K27me3 (inactive) exclusively occupies those genes that are repressed during a cells trip down a particular differentiation path (Fig. 3). Although this is not complete, these findings suggest that maintenance of pluripotency is in some capacity regulated by epigenetic processes.

### 1.2.4. Nanog and Pluripotency

In 2003, the overexpression of the gene Nanog was shown to help maintain ESCs pluripotency even after removal of LIF (Chambers and Smith; Yamanaka 2006). Mouse Nanog encodes a 305 amino acid protein consisting of 3 distinct domains; an N-terminal

domain, a homeodomain, and a C-terminal domain (Figure 4) (Do, Lim et al. 2007). The Nanog homeodomains sequence shows some (less than 50%) similarity with the homeodomain of members of the NK2 family of homeoproteins. Nanog shows no similarity with any other protein discovered to date, making it a novel transcription factor. Since its discovery, Nanog has been a major focus in the field. It has been shown to both positively and negatively regulate distinct sets of genes involved in pluripotency and differentiation of stem cells, the precise mechanisms of these interactions remains to be unknown. Attempts to create Nanog null embryos were unsuccessful; homozygous embryos appeared to consist entirely of disorganized extraembryonic tissues with no discernible epiblast or extraembryonic ectoderm (Mitsui, Tokuzawa et al. 2003). When cultured on gelatin-coated plates, ICM of 3.5 dpc Nanog null blastocysts failed to proliferate (Mitsui, Tokuzawa et al. 2003). Chambers et al, created a temporal Nanog null cell by utilizing a Cre-loxP system where the nanog can be excised, these cells showed spontaneous differentiation to primitive endoderm (Chambers, Colby et al. 2003).

### 1.2.5. Nanog Interactions With Other Proteins

Although Nanog is a crucial regulator of stem cell maintenance, it is not solely responsible for stem cell maintenance. Other transcription factors are heavily involved, including Oct4 (also known as Pou5f1) and Sox2. Oct4 is also a homeodomain transcription factor and its loss results in inappropriate differentiation of the inner cell mass and ESC into trophoectoderm. On the other hand, overexpression of Oct4 causes differentiation into primitive endoderm and mesoderm (Niwa 2007). These contrasting results suggest that it is not only its presence or absence, but, that precise Oct4 levels are necessary for maintaining pluripotency. Oct4 has also been shown to regulate gene

expression by its interaction with other transcription factors with in the nucleus. One such interaction is that between Oct4 and the high mobility group (HMG)-box transcription factor Sox2 (Boyer, Lee et al. 2005). Sox2 has been shown to play an important role in the maintenance of ES cells and also lineage specificity upon differentiation. Sox2, however, is not restricted to the pluripotent cells as Oct4 and Nanog have been found to. Sox2 also has been found in early neural lineages (Avilion, Nicolis et al. 2003). Nanog, Oct4, and Sox2 are the earliest-expressed genes known to be responsible for maintaining the ESC state. Because of each of their distinct roles, it can be assumed that they function in separate pathways, but that may converge to regulate and maintain common genetic targets critical in both stem cell maintenance and early cell fate decisions. Another group of proteins that is regulated by Nanog is the Gata family of proteins. A balance between Gate4 and Gata6 exists between Nanog. Gata4 and Gata6 are transcription factors involved in endodermal differentiation (Capo-chichi, Rula et al. 2005). In the absence of Nanog, Gata4 and Gata6 are upregulated, and over expression of Gata4 or Gata6 leads to primitive endoderm (Capo-chichi, Rula et al. 2005).

### 1.2.6. Nanog Transcriptional Regulation

Nanog belongs to a core set of regulatory proteins responsible for ESC maintenance. Nanog not only prevents differentiation, but it also actively maintains pluripotency by its interactions with many Nanog targets (Mitsui, Tokuzawa et al. 2003), although the molecular mechanism by which Nanog performs these actions are still not entirely understood. Mitsui et al suggest that Nanog maintains self renewal of ES cells by transcriptional repression of critical differentiation genes (such as gata4 and gata6) (Mitsui, Tokuzawa et al. 2003). Nanog has also been shown to be a transactivator, with

the potential to not only activate critical pluripotency genes, but also itself (Pan and Pei 2003). Nanogs C and N terminal have been shown to have great transactivation potential (Wang, Ma et al. 2008). The N terminal of Nanog is rich in Ser and Thr acidic residues, indicative of a transactivation motif, and has been shown to have a 35 fold increase on transactivation effects. The C terminal of Nanog showed no apparent transactivation motif but still showed to contain a 240 fold increase in transactivation (Pan and Pei 2003). It was shown that the aromatic residues in the C terminal end of the C terminus of Nanog are largely responsible for this effect (Wang, Ma et al. 2008), but the direct mechanism is still not understood.

#### 1.2.7. Nanog Cellular Localization

Nanog is a nuclear transcription factor, and is localized to the nucleus of ESCs. It has been shown that the homeodomain of Nanog contains a nuclear localization signal (NLS). Mutational analysis located two NLS motifs at the C and N terminal of the homeodomain, and showed that both were necessary for complete nuclear localization and maintenance of ES cell like morphology (Do, Lim et al. 2007). Constructs containing a series of deletions and site-directed mutagenesis showed that an intact homeodomain (residues 95-154) (Fig. 4) was both sufficient and necessary for nuclear localization of Nanog protein (Do, Lim et al. 2007).

### 1.3. Transcriptional Regulation

#### 1.3.1. GSK3*β* and Nanog Regulation

GSK3*β*, is a serine-threonine kinase shown to be important in stem cell biology (Cartwright, McLean et al. 2005). GSK3*β* is inactive and phosphorylated at Serine 9, in self-renewing, pluripotent mESC. During differentiation Serine 9 phosphorylation

decreases (Cartwright, McLean et al. 2005), and GSK3$\beta$ is translocated to the nucleus (unpublished data, Bechard and Dalton). Inhibition of GSK3$\beta$ by BIO has been shown to maintain pluripotency in ESCs (Storm, Bone et al. 2007). GSK3$\beta$ is a member of the PI3K pathway, which has previously been discussed, and is necessary for mESC maintenance and pluripotency. Inhibition of the PI3K pathway by LY294002 led to the reduction in the ability of LIF to maintain self-renewal, with cells simultaneously differentiation and spontaneously differentiation and adopting different morphologies (Paling, Wheadon et al. 2004). Inhibition of PI3K also decreased basal phosphorylation of AKT, GSK3$\beta$ and S6 proteins, had no effect on LIF-induced phosphorylation of STAT3 at $Try^{206}$, and increased LIF-induced phosphorylation of ERKs (Paling, Wheadon et al. 2004). Also proposed from this group was that PI3K signaling regulates Nanog. Throughout their paper they show that blocking the PI3K pathway, with either LY and by genetic tools, resulted in decreased expression of RNA for the homeodomain of the transcription factor nanog and decreased Nanog protein levels (Paling, Wheadon et al. 2004). They also show that blocking GSK3$\beta$ by BIO causes Nanog levels to remain high (Paling, Wheadon et al. 2004; Storm, Bone et al. 2007); however, they fail to show any direct correlation. It remained unclear if the inhibition of GSK3$\beta$ was causing the retention of Nanog protein, or, if Nanog levels were remaining high because BIO was causing the cells to maintain pluripotency and self-renewal. It was this ambiguity, along with other data, that prompted us to take a closer look at this relationship between GSK3$\beta$ and Nanog.

# Chapter 2. MATERIAL AND METHODS

## 2.1 Abbreviations

| | |
|---|---|
| $A_{260}$ | Absorbance at 260 nm |
| BIO | 6-bromoindirubin-3'-oxime |
| *β*-ME | *β*-Mercaptoethanol |
| BSA | Bovine Serum Albumin |
| cDNA | Complementary DNA |
| CHX | Cycloheximide |
| CIP | Calf intestinal Phosphatase |
| dATP | deoxyadenosine triphosphate |
| dCTP | deoxycytosine triphosphate |
| dGTP | deoxyguanosine triphosphate |
| dTTP | deoxythymidine triphosphate |
| DAPI | 4',6-diamidino-2-phenylindole |
| EDTA | Ethylenediaminetetracatic acid |
| EtBr | Ethidium Bromide |
| DMEM | Dulbecco's Modified Eagles Medium |
| DMSO | Dimethylsulphoxide |
| DNA | Deoxyribonucleic acid |
| DPBS | Dulbecco's Phosphate Buffered Saline |
| DTT | Dithiothreitol |
| *E.coli* | *Escherichia coli* |
| ESC | Embryonic Stem Cell |

| | |
|---|---|
| EtOH | Ethanol |
| FBS | Fetal Bovine Serum |
| g | Gram |
| HRP | Horse Radish Peroxidase |
| ICM | Inner Cell Mass |
| kb | Kilo base pair |
| kd | Kilo Dalton |
| KSR | Knockout Serum Replacement |
| L | Liter |
| LIF | Leukemia Inhibitory Factor |
| M | Molar |
| mM | milliMolar |
| $\mu$M | microMolar |
| $\mu$g | microgram |
| $\mu$l | microliter |
| mAmps | Milliamps |
| min | Minute |
| mg | Milligram |
| ml | Milliliter |
| mRNA | Messenger RNA |
| mESC | Murine Embryonic Stem Cell |
| meBIO | 1-methyl-6-bromoindirubin-3'-oxime |
| MG132 | Nbenzyloxycarbonyl-Leu-Leu-leucinal |

| | |
|---|---|
| MW | Molecular Weight |
| PAGE | Polyacrylamide Gel Electrophoresis |
| PBS | Phosphate Buffered Saline |
| PCR | Polymerase Chain Reaction |
| PFA | Paraformaldehyde |
| RNA | Ribonucleic Acid |
| rpm | Revolutions per Minute |
| SDS | Sodium Dodecyl Sulphate |
| TAE | Tris Acetate EDTA |
| To-pro | Monomeric Cyanine Nucleic Acid Stains |
| tRNA | Transfer RNA |
| Tween-20 | Polyoxyethylene-Sorbitan Monolaurate |
| U | Units |
| UV | Ultraviolet |
| V | Volts |

## 2.2 Tissue Culture

### 2.2.1 Materials

| | |
|---|---|
| Ampicillin | Sigma |
| *β*-ME | Gibco |
| DMEM | Cellgro |
| DMSO | Sigma Aldrich |
| Ethanol | Fisher |
| FBS | Invitrogen |

| | |
|---|---|
| Gelatin | Sigma |
| KSR | Gibco |
| L-Broth | Cellgro |
| L-Glutamine | Cellgro |
| Methanol | Fisher |
| Penicillin/Streptomycin | Cellgro |
| Puromycin | Sigma |
| Sodium Pyruvate | Cellgro |
| Trypan Blue | Cellgro |
| Trypsin | Cellgro |

### 2.2.2 Tissue Culture Plasticware

| | |
|---|---|
| 6 well trays | BD Falcon |
| 96 well trays | BD Falcon |
| 10 cm plates | BD Falcon |
| Pipettes | Corning |

### 2.2.3 Buffers

| | |
|---|---|
| PBS | Cellgro |
| DPBS | Cellgro |

### 2.2.4 Solutions

| | |
|---|---|
| PBS/Gelatin | 0.2% gelatin in DPBS |

### 2.2.5 Cell Culture Medium

| | |
|---|---|
| mESC Complete Media | DMEM containing high glucose supplemented with 10% FBS, 10% KSR, |

| | |
|---|---|
| | 1mM L-glutamine, 1mM Sodium Pyruvate, Pen/Strep, 0.1mM $\beta$-Me and 1000U/ml LIF |
| mESC Incomplete Media | DMEM containing high glucose supplemented with 10% FBS, 10% KSR, 1mM L-glutamine, 1mM Sodium Pyruvate, Pen/Strep, and 0.1mM $\beta$-Me |

### 2.2.6 Cell Lines

All cells were maintained at 37°C in 10% $CO_2$

| | |
|---|---|
| R1: | Derived from the ICM of the pre-implantation Sv x 129/Sv-CP F1 3.5 blastocyst. (Nagy, Rossant et al. 1993) |

### 2.2.7 Miscellaneous

| | |
|---|---|
| Amersham Hyperfilm ECL | GE Healthcare |
| Cryo 1°C Freezing Container | Nalgene |
| Plate Scraper | VWR International |
| Accuspin I Centrifuge | Fisher Scientific |
| Microcentrifuge 5417C | Eppendorf |

## 2.3 Tissue Culture Methods

### 2.3.1 Gelatinized Tissue Culture Plates

All tissue culture dishes and plates used for mESCs were gelatinized with 0.2% (w/v) gelatin in PBS. Plates were covered with gelatin solution and left for at least 20 minutes at room temperature. The gelatin solution was removed and then plate was washed with PBS immediately before use.

### 2.3.2 Determination of Cell Number

Cells were harvested as described (2.3.5). A 10 µl aliquot of the single cell suspension was added to 10 µl of trypan blue. Cell numbers were counted under 100x phase contrast magnification using a hemocytometer. Trypan blue-stained dead cells were omitted from the cell count.

### 2.3.3 Preparation of Cell Lines for Storage

Cells were harvested to a single cell suspension as described in (2.3.5) with the following alteration. Cells were resuspended in a solution of 50% FBS, 50% mES complete medium solution. Then, an equal volume of 80% mES complete medium, 20% DMSO dropwise. The final concentration was $1x10^6$ cells/ml put into 1ml aliquots for freezing. Cells were placed in the Mr. Frosty for 4-6 hours in the -80°C then transferred to liquid nitrogen for long term storage.

### 2.3.4 Thawing Stored Cell Lines

Frozen cells were thawed in a 37°C water bath then diluted in 10 ml of fresh culture medium and spun at 180 x *g* for 4 minutes. Cells were then resuspended in the appropriate medium and placed a gelatinized 10 cm dish. Thawed cells were placed at 37°C, 10% $CO_2$, in a humidified incubator. The following day, medium was replaced with fresh medium.

### 2.3.5 Maintenance of mESCs

R1 mESCs were cultured, in the absence of feeders, on tissue culture grade plastic pre-treated with 0.2% gelatin/PBS (2.3.1). Semi-confluent mESC plates were washed once in PBS before the addition of 0.05% trypsin (3ml) at 37°C for 3 minutes. mESCs were removed from the dish and forced into single cell suspension with pipetting and

transferred into 5 ml complete mES medium. The cells were spun at 180 x *g* for 4 min, gently resuspended in 10 ml of mES complete medium and re-seeded on to pre-gelatinized 10 cm plates at a cell density ranging from $3.5x10^5$-$5x10^5$ cells per plate, and maintained at 37°C, 10% $CO_2$ as described in (Stead E 2002). Cells were passaged every 3-4 days for a maximum of 30. mESCs were maintained in mES complete medium.

### 2.3.6 Harvesting Cells for Protein Extraction

At the desired time point plates were washed 2x with PBS, harvested by scraping and cells were gently resuspended in 5 ml of PBS. Cells were then spun at 180 x *g* for 4 minutes. PBS was aspirated and the cell pellets were frozen at -80°C.

### 2.3.7 Treatment of mESCs with MG132

R1 mESCs and generated cell lines were maintained in mESC complete medium or incomplete medium. For treatment of mESCs with MG132 cells were grown in the mES complete or incomplete medium. 4-6 hours before the cells were harvested MG132 was added to the plate at a final concentration of 5$\mu$M. Plates were washed 2x with PBS, scraped and spun at 180 x *g* for 4 minutes. Cell pellets were snap frozen on dry ice and stored at -80°C. Whole cell extracts were prepared and subject to western analysis as described (2.5.11)

### 2.3.8 Treatment of mESCs with BIO

R1 mESCs and created cell lines were maintained in mESCs complete medium or incomplete medium. For treatment of mESCs with BIO (or meBIO) cells were grown in mESC complete of incomplete medium up to 3 days with BIO at a final concentration or 2$\mu$M. Plates were washed 2x with PBS, harvested by scraping, and spun at 180 x *g* for 4

minutes. Cell pellets were snap frozen on dry ice and stored at -80°C. Whole cell extracts were prepared and subject to western blot analysis as described (2.5.11)

### 2.3.9 Treatment of mESCs with Cycloheximide

R1 mESCs and created cell lines were maintained in mESC complete medium, cells were treated with 2$\mu$M cycloheximide in DMSO, and harvested by scraping at various time points. Cell pellets were snap frozen on dry ice and stored at -80°C. Whole cell extracts were prepared and subject to western analysis as described (2.5.11)

## 2.4 Molecular Biology

### 2.4.1 Chemicals

All chemicals were of molecular biological grade and the highest purity available.

| | |
|---|---|
| Agar | Bio-Rad |
| $\beta$-ME | Sigma |
| Chloroform | Fisher |
| DTT | Sigma Aldrich |
| EtBr | Sigma |
| Ethanol | Fisher |
| EDTA | Fisher |
| Ethanol | Fisher |
| Glycine | Bio-Rad |
| Formaldehyde | Sigma |
| L-Broth | Cellgro |
| Methanol | Fisher |
| Phenol | Sigma |

| | |
|---|---|
| Tween 20 | Fisher |
| SDS | Fisher |
| Tris-HCL | Fisher |
| Triton X-100 | Fisher |
| Skim Milk | Bio-Rad |

### 2.4.2 Enzymes

Restriction endonucleases supplied by New England Biolabs

| | |
|---|---|
| Calf Intestinal Phosphatase: | Promega |
| DNAse I: | New England Biolabs |
| Proteinase K: | Sigma |
| RNAse A: | Sigma |
| T7 RNA polymerase: | New England Biolabs |
| T4 DNA ligase: | New England Biolabs |

All enzymes were stored to the manufacturers' specifications

### 2.4.3 Buffers

| | |
|---|---|
| RIPA Buffer | 50mM Tris pH 7.4, 1% NP4O, 0.5% DOC, 150mM NaCl, 1mM EDTA, 0.1% SDS, 1mM DTT, protease inhibitor, phosphatase inhibitor |
| Western Transfer Buffer | 12.5mM Tris, 100mM Glycine, 20% methanol |
| Western SDS PAGE Running Buffer | 192mM Glycine, 25 mM Tris, 0.1% SDS |

| | |
|---|---|
| Western TBST Wash Buffer | Bio-Rad |
| Laemmli Buffer | Bio-Rad |

### 2.4.4 Molecular Biology Kits

| | |
|---|---|
| Plasmid Purification | Qiagen |
| QuikChange Site-Directed Mutagenesis Kit | Stratagene |
| Qiaquick Gel Extraction Kit | Qiagen |

### 2.4.5 DNA Molecular Weight Markers

| | |
|---|---|
| 100 base pair DNA ladder | New England Biolabs |
| 1 kb pair DNA ladder | New England Biolabs |

### 2.4.6 Protein Molecular Weight Markers

| | |
|---|---|
| Precision Plus Protein Dual Color Standards | Bio-Rad |

### 2.4.7 Cloning Vectors

pBluescript II SK (+): Stratagene. pBluescript II SK (+) plasmid DNA was linearized (2.5.9) with appropriate restriction enzyme(s), phenol/chloroform extracted, Ethanol precipitated and treated with CIP (2.5.3) to inhibit re-ligation of the vector alone.

### 2.4.8 Cloned Sequence

*Nanog*

### 2.4.9 Oligonucleotides

| | |
|---|---|
| NanSeq-F1 | 5’ – ATGAGTGTGGGTCTTCCTG -3’ |
| NanSeq-F2 | 5’ – AGCTGTGTGCACTCAAGG – 3’ |
| NanSeq-F3 | 5’ – AGACTTGGACCAACCCAC – 3’ |
| NanSeq-R1 | 5’ – CACCTGGTGGAGTCACAG – 3’ |
| NanSeq-R2 | 5’ – GTTATGGAGCGGAGCAGC – 3’ |
| NanSeq-R3 | 5’ – TCCTGCCACCGCTTGCAC – 3’ |

NanSeq-R4 5’ – GAAGAGGCAGGTCTTCAG – 3’

### 2.4.10 Bacterial Strains

The *E.coli* DH5α strain was used as a host for all recombinant plasmids

DH5αT1 Competent Cells (Invitrogen)

### 2.4.11 Bacterial Growth Methods

Growth L-broth media (Cellgro) plus appropriate antibiotic

Solid Media: Agar plates were prepared by adding 1% Bacto-tryptone, 0.5% yeast extract, 1% NaCl,, 1.5% Bacto-agar, Ampicillin (100µg/ml) was added for growth of transformed bacteria and to maintain selective pressure for recombinant plasmids.

### 2.4.12 Miscellaneous Materials

Vectorshield Vectorlabs

## 2.5 Molecular Methods

### 2.5.1 Gel Electrophoresis

Agarose gel electrophoresis (0.8%-1% in 1x TAE) was carried out using horizontal gels prepared by pouring 50ml of agarose solution into the glass plate. 10$\mu$g/ml EtBr was added to the liquid agarose. Agarose gels were allowed to set at room temperature prior to being submerged in 1x TAE in a gel electrophoresis system (Bio-Rad). DNA loading dye (New England Biolab) was then added to DNA samples. Samples were loaded into wells within the agarose gel and electrophoresed at 90 mA. Gels were photographed under medium UV light using a Fotodyne Incorporated Imager. Appropriate molecular size of DNA fragments were assessed by comparison with EtBr stained DNA molecular weight markers.

### 2.5.2 Isolation of DNA Fragments from Gels

Linear DNA fragments were run on appropriate percentage TAE agarose gels and visualized under long wave UV light. Bands were removed from the preparative gels using a clean scalpel blade and purified from the agarose using the Qiaquick Gel Extraction Kit (Qiagen) according to the manufacturers' instructions.

### 2.5.3 Removal of 5' Phosphate Groups from Vector DNA Fragments

The 5' phosphate groups were removed from DNA ends by treatment with CIP prior to gel purification. The reaction was initiated by the addition of 5$\mu$l of 10x CIP buffer and 1$\mu$l (1U/$\mu$l) of CIP. The reaction was incubated at 37°C for 30 minutes. Dephosphorylated vector DNA was then electrophoresed (2.5.1) on a 1% TAE gel and purified using the Qiagen Gel Extraction Kit (2.5.2)

### 2.5.4 Transformation of Competent Bacteria With Plasmid DNA

Transformation of DNA into competent cells, were done as described by the manufacturers' instructions for One Shot Max Efficiency DH5α-T1 Competent Cells (Invitrogen).

### 2.5.5 Selection of Positive Transformants

Transformed bacteria were then streaked onto LB Ampicillin (50$\mu$g/ml) plates (2.4.11) and left in a 37°C incubator overnight. Colonies were then picked and used to inoculate Amp Broth (2.4.11) for amplification and DNA extraction.

### 2.5.6 Rapid Small Scale Mini-preparation of Plasmid DNA

Plasmid DNA purification was done according to the manufacturers' instructions in the QIAprep Spin Miniprep Kit (Qiagen) and a microcentrifuge (Eppendorf).

### 2.5.7 Midi-preparation of Plasmid DNA

Plasmid DNA purification was done according to the Qiagen Plasmid Purification Midi Kit (Qiagen)

### 2.5.8 DNA Sequencing

Purified DNA was resuspended at an appropriate concentration (150 ng/$\mu l$ for plasmids, and about 15 ng/$\mu$l for PCR products in 20 $\mu$l of HPLC grade water) and sent to the Office of Instrumental Biology Laboratory, at the University of Georgia, for sequencing analysis.

### 2.5.9 Restriction Digestion Analysis of plasmid DNA

Analytical digestion of DNA with restriction endonucleases was carried out for 1 hour to overnight at recommended temperatures. DNA was digested in 1x restriction enzyme buffer and 0.5 $\mu$g of DNA to 5-10 U of enzyme in a total volume of 20 $\mu$l. All enzymes were stored at -20°C, and used to manufacturers' specifications.

### 2.5.10 Construction of Stable Cell Lines

Verified sequences were ligated into the expression vector pCAGIPuro (Chambers and Robertson, 1997) using T4 DNA Ligase (New England Biolabs) as instructed in manufacturers specifications and left at room temperature for 3 hours, and then transformed into R1 cells using Lipofectamine 2000 (Invitrogen) as instructed by manufacturers specifications.

### 2.5.11 Cell Line Selection

Cells were plated on gelatinized plates with complete ESC media and allowed to grow over night. At day 2 puromycin was added to the media at 1µg/ml and cells were grown under Puromycin Selection for 2-3 weeks. Colonies were then picked and clonal cell lines were expanded to a specified density.

### 2.5.12 Preparation of Whole Cell Extracts

Harvested cell pellets were extracted with 2 volumes of RIPA buffer on ice for 30 minutes with occasional pipetting. Cell extract supernatant was collected by centrifugation at 375 x *g* for 2 minutes at 4°C. Protein concentrations were then determined by Bradford Assay.

### 2.5.13 Western Blot Analysis

10-20 $\mu$g of protein per lane was subject to PAGE in western running buffer, using a 10% Tris-HCl pre-cast gel (BIO-RAD) at 20mAmps for 2-3 hours. Proteins were then transferred to a nitrocellulose membrane (BIO-RAD) in western transfer buffer at 250mAmps for 1 hour. Membranes were blocked with 1% skim milk/TBST for 1 hour at room temperature before the addition of primary antibody, 1:1000, in 0.5% skim milk/TBST. Filters were then incubated overnight at 4°C with gentle rocking. Filters were washed 3x for 10 minutes with TBST wash buffer before the addition of HRP conjugated secondary antibodies (DAKO), 1:2000, in 0.5% skim milk/TBST for 1 hour. Filters were then washed 3x for 10 minutes with TBST. Fliters were developed with ECL reagent from Amersham and exposed to X-ray film (GE Heathcare).

### 2.5.14 Immunoprecipitation Analysis

Protein A sepharose beads were pre-blocked with 1% BSA, and conjugated to Nanog antibody by overnight incubation and spinning at 4°C. 300-500 $\mu$g of extracted protein was added to pre-blocked protein A sepharose beads, and rotated at 4°C for 1 hour. Tubes were then spun at 375 x *g* for 1 min and the supernatant was removed. Beads were washed 3x with RIPA buffer. Appropriate volume of Laemmli Sample Loading Buffer was then added to beads and boiled for 2 minutes at 95°C to remove

protein. Tubes were spun at 375 x *g* for 1 min and protein supernatant was collected for western blotting.

## 2.6 Histological Analysis

| 2.6.1 Primary Antibodies | Vendor (Catalog #) |
|---|---|
| c-myc | Cell Signaling (9402) |
| CDK2 | Santa Cruz Biotechnology (6248) |
| GSK3β | BD Transduction Laboratory (610202) |
| GSK3β phospho S9 | Cell Signaling (9336) |
| HA | Cell Signaling (2367) |
| OCT-4 | Santa Cruz Biotechnology (8629) |
| Nanog | Cosmo Bio Co (RCAB0002P-F) |
| p-Ser | Sigma (P3430) |
| p-Thr | Sigma (P3555) |

| 2.6.2 Secondary Antibodies | Vendor (Catalog #) |
|---|---|
| Goat anti rabbit, HRP conjugated | DAKO (P0448) |
| Rabbit anti mouse, HRP conjugated | DAKO (P0161) |

| | |
|---|---|
| Rabbit anti goat, HRP conjugated | DAKO (P0449) |
| AlexaFlour goat anti mouse 488 nm | Molecular Probes (A21042) |
| AlexaFlour goat anti mouse 594 nm | Molecular Probes (A11005) |
| AlexaFlour goat anti rabbit 488 nm | Molecular Probes (A11008) |
| AlexaFlour goat anti rabbit 633 nm | Molecular Probes (A21070) |
| AlexaFlour donkey anti rabbit 488 nm | Molecular Probes (A21206) |
| AlexaFlour donkey anti mouse 488 nm | Molecular Probes (A21202) |

| **2.6.3 Nuclear Dyes** | **Vendor (Catalog #)** |
|---|---|
| DAPI | Invitrogen (D1306) |
| To-Pro | Molecular Probes (T3605) |

| **2.6.4 Conjugated Beads** | **Vendor (Catalog #)** |
|---|---|
| Protein A Sepharose Beads | Sigma (17-5280-01) |
| EZview Red Anti-HA Affinity Gel | Sigma (E6779) |

### 2.6.5 Immunofluorescence Cell Staining

mESCs cultured previously as described (2.3.5) were plated on gelatin coated chamber slides at a cell density of 2.5 x $10^5$ cells/ml. Medium was aspirated and cells were washed with PBS, and then fixed for 5 minutes at room temperature with 4% PFA. PFA

was then aspirated and the cells were washed 2x with PBS. Cells were then permeabilized for 5 minutes at room temperature with 0.2% Triton X in PBS. Cells were washed 2x in PBS and blocked for 1 hour in 10% goat serum at room temperature. Cells were then incubated with primary antibody, 1:100 in 10% goat serum overnight at 4°C. Cells were washed 2x with PBS before incubation with secondary antibody at 1:250 in 10% goat serum for 1 hour at room temperature in the dark. Cells were then washed with To-pro nuclear dye, 1:300 in PBS. Chamber slides were mounted with Vectashield (Vectorlabs) mounting media and coverslips were sealed with nail polish. Immunofluorescence was visualized on Leica DM 6000 B upright microscope or Zeiss LSM Meta 10 confocal microscope.

## Chapter 3. NANOG LOCALIZATION

### 3.1 Nanog Localization in mESCs

Nanog is a nuclear transcription factor known to interact and regulate the activity of many other proteins important in mESC maintenance. R1 mESCs, grown in the presence of LIF (complete mES media), exhibit elevated Nanog levels predominantly localized to the nucleus (Fig.5). Upon removal of LIF, Nanog levels began to decrease; by day 2 Nanog levels were significantly lower, and by day 3 Nanog has been almost completely degraded (Fig 5). This data is consistent with other reports, however, little was known about the mechanism Nanogs degradation and its elucidation became one of the topics of interest in this project.

### 3.2 Nanog Localization in Rb Triple knockout cell line

In a previous project I had been looking at an Rb, p107, and p130 triple knock out cell line; investigating cell cycle related interactions in ES cells. Retinoblastoma protein is a tumor suppressor protein involved in cell cycle regulation. Rb belongs to a family of proteins called pocket proteins (Rb, p107, and p130). pRb prevents the cell from replicating damaged DNA by preventing its progression along the cell cycle through G1 into S phase (Korenjak and Brehm 2005). While characterizing the properties of this cell line (obtained from Floris Foijer), it was observed that these cells seemed to have a more flattened morphology and differentiate slower than the R1 mESC. Upon removal of LIF it was observed that Nanog was found through out the entire cell (Fig.6), and not strictly the nucleus, as had been previously reported (Fig. 5). This peculiar finding prompted us to investigate if cytoplasmic Nanog was a phenomenon specific to this cell line. We hypothesized that Nanog could be going through a cytoplasmic transition before its

degradation in other ESC lines. We also hypothesized that this event had never been observed before because of the transient nature of this occurrence, and the possible degradation of Nanog protein immediately following its export from the nucleus to the cytoplasm.

### 3.3 Nanog Localization during proteasome inhibition

Since the Rb TKO mESCs were differentiating at a slower rate than the R1 mES cells, we inquired if cytoplasmic Nanog could be observed in the wild type R1 cell line if we could someway slow the rate of the cells spontaneous differentiation upon removal of LIF. To address this question we added MG132, a proteasome inhibitor, with the idea that blocking Nanog degradation may allow the accumulation of Nanog in the cytoplasm to be detected. The proteasome is thought to have different distinct catalytic activities. One firmly established and well characterized of these activities is the chymotrypsin-like activity, in which the proteasome cleaves peptides at the carboxyl side of Tyr, Trp, and Phe residues. The peptide aldehyde, Benzyloxycarbonyl-L-Leucyl-L-Leucyl-L-Leucinal (MG132), greatly reduces the chymotrypsin-like activity of the proteasome on ubiquitin-conjugated proteins in mammalian cells and permeable strains of yeast (Fenteany and Schreiber 1996). Since the direct mechanism of Nanog degradation is unknown, we hypothesized that it could be through ubiquitin mediation, and that addition of MG132 could block its degradation. Addition of MG132 (5 $\mu$M, 4 hours before harvesting) to R1 ESCs grown in the presence and absence of LIF showed not only a retention of Nanog protein, but also the appearance of some cytoplasmic Nanog (Fig.7). This led us to hypothesize that Nanog accumulates in the cytoplasm prior to its degradation during differentiation.

### 3.4 Nanog Localization during inhibition of GSK3β

This preliminary evidence of cytoplasmic Nanog with the addition of MG132 caused us to hypothesize that cytoplasmic Nanog could be a prerequisite for Nanog degradation during differentiation. This led to our investigation of Nanog degradation *in vivo*.

The PI3K pathway and GSK3*β* had both been implicated in differentiation and Nanog regulation, but this had not been entirely validated (Storm, Bone et al. 2007). This, along with other data in our lab, prompted us to consider GSK3*β* as a possible player responsible in Nanogs translocation to the cytoplasm and its possible degradation.

We tested this hypothesis by investigating the effect of BIO, a potent GSK3*β* inhibitor, on Nanog levels during differentiation. It is shown in Figure 8 that the addition of BIO (2μM) to R1 mESCs resulted in the maintenance of high nuclear Nanog protein levels even after removal of LIF. This result led us to hypothesize that GSK3*β* could be responsible or have a possible role in Nanog degradation. Addition of both MG132 and BIO showed an increase in the stability of Nanog protein after removal of LIF (Fig. 9). This was consistent with observations from the addition of BIO alone, however, simultaneous addition of MG132 did not show any cytoplasmic Nanog, which led us to hypothesize that active GSK3*β* could be involved, or necessary, in Nanog translocation to the cytoplasm and its eventual degradation during differentiation.

## Chapter 4. MODIFICATIONS OF NANOG PROTEIN

### 4.1 Modification of Nanog due to proteasome inhibition

We next hypothesized that the cytoplasmic form of the Nanog protein could have some sort of modification, and we wanted to observe if there were any detectable changes or shifts in Nanog protein bands on a Western Blot. To further investigate this question, whole cell lysates were made from R1 cells grown in the presence and absence of LIF, and with and without MG132. Whole cell lysates were subjected to SDS-PAGE and Western blot analysis. Nanog levels were significantly decreased after 2 and 3 days without LIF, this appeared to be rescued by the addition of MG132 (Fig. 10), consistent with the correlating immunofluorescence data (Fig. 7). Nanog protein appears at a molecular weight of around 39 kD on an immunoblot, and exists as a doublet (Fig. 10). We found that addition of MG132 not only rescued some of the total amount of Nanog protein, but also increased the amount of protein in the upper band form of the doublet. We wanted to further investigate the composition of this upper band (higher molecular weight) form of Nanog.

### 4.2 Nanog is a Phosphoprotein

We hypothesized that the upper band form of the Nanog doublet appearing due to MG132 treatment, could be representative of the Nanog found to be localized to the cytoplasm under that same conditions. The shift of the upper band form of the doublet was about 2-3 kD. This size shift is comparable to a shift due to phosphorylation by GSK3$\beta$ in other proteins (Cai 2006). Nanog had previously been shown to exist as a phosphoprotein (Yates and Chambers 2005), and we wanted to investigate this further to distinguish if the upper band found in the MG132 samples could be due to Nanog

phosphorylation. Nanog IP's were preformed, and eluted protein was immunoblotted, and probed with a phospho-serine antibody (Fig. 11). We reported that ESCs grown in the presence of LIF, with MG132 treatment, showed a band representing Nanog phosphorylation. We show that cells grown in the absence of LIF, without MG132, did not show a band, indicating that there was not any Nanog phosphorylation. However, we do show that cells grown in the absence of LIF, with MG132 treatment, show a band indicating that phosphorylated Nanog does exist when proteasomal degradation is inhibited. These results led us to postulate that phosphorylation of Nanog could be linked to its degradation, and therefore, would only be visible transiently, and at a time of early differentiation. Also, leading us to hypothesize that phospho-Nanog could be the Nanog we see localized to the cytoplasm during MG132 treatment, and the upper band form of the Nanog doublet.

# Chapter 5. NANOG-HA MUTANTS

## 5.1 Nanog-HA Mutants Localization

Since we had established a correlation between Nanog phosphorylation and degradation, we began to focus on a more direct way to study this interaction. Other data in our lab had shown that Nanog contained a conserved GSK3$\beta$ phosphorylation sequence of S/TXXXS/TP with in the N terminal of the Nanog protein sequence (Fig. 4). Phosphorylation by this serine-threonine kinase has been shown before to be an inactivating phosphorylation with such proteins as: c-Myc, $\beta$-Catenin, and Glycogen Synthase (Cai 2006). This led us to hypothesize that GSK3$\beta$ could be the kinase responsible for Nanog phosphorylation and involved in its ultimate degradation. To further investigate this potential interaction, Nanog-HA cell lines were created in which the conserved serine (S52) and threonine (T48) residues in the GSK3$\beta$ phosphorylation sequence were mutated to alanine residues. The pCAGIPuro expression vector (Chambers I 1997) was used to create a construct; wild type Nanog ($Nanog^{wt}HA$), and two mutated forms of Nanog ($Nanog^{T48A}HA$, $Nanog^{T48A/S52A}HA$), were inserted along with a C terminal triple HA tag (2.5.10). Cell lines were constructed, and grown under antibiotic selection (2.5.11) for 3 weeks before colonies were selected. Cell lines expressing appropriate and equivalent protein levels as compared to endogenous Nanog were chosen (data not shown). The expression vector was under the control of the hybrid CMV β-actin (CAG) promoter, which retains activity during differentiation. Two mutant cell lines were created with point mutations within the GSK3$\beta$ phosphorylation site, a single T48A mutant, and a double T48A/S52A. This allowed us to see how a form of Nanog, which was not able to be phosphorylated by GSK3$\beta$ would respond under the

previous conditions that had been tested. Nanog$^{wt}$HA immunofluorescence confocal imaging revealed that the cell line expressing the HA-tagged Nanog expression was similar to that of endogenous Nanog, and was also correctly localized to the nucleus, opposing any doubts that the assembly of the construct would interfere with classical Nanog function or localization (Fig. 12). Figures showed that the Nanog panels represent endogenous Nanog, and HA represent the HA tagged form of Nanog (WT, T48A, or T48A/S52/A). In the single mutant cell line, Nanog$^{T48A}$HA, we observed that the mutant form of Nanog was more stable upon removal of LIF compared to endogenous Nanog, and there was cytoplasmic localization of Nanog with the addition of MG132 (Fig.13). Nanog$^{T48A/S52A}$HA shows an even smaller decrease in signal when compared to endogenous Nanog upon removal of LIF, and cytoplasmic localization (Fig. 14). Also, the double mutant showed some cells in the colony to have complete nuclear exclusion of the tagged Nanog. These results verified our hypothesis that GSK3$\beta$ is involved in Nanog stability. However, the mutated forms of Nanog that were unable to be phosphorylated by GSK3$\beta$ still showed some cytoplasmic localization upon addition of MG132. From this data we conclude that inhibition of Nanog phosphorylation, by mutation of the GSK3$\beta$ phosphorylation sequence, is not sufficient to block cytoplasmic translocation of Nanog during differentiation.

**5.2 Nanog-HA Mutants Protein Modification**

To further validate our hypothesis of GSK3$\beta$'s importance for Nanog degradation, immunoprecipitations and western blots were done in parallel with the previous cell lines and conditions. In cells grown in the absence of LIF for 2 days, the Nanog$^{wt}$HA cell line showed a doublet (Fig. 15), this was consistent with what had been observed in the R1

cell line (Fig. 10). Tagged mutant cell lines began to show an increase in a lower band form of this doublet (Fig. 15). The Nanog$^{T48A/S52A}$HA cell line shows an increase in a lower band form of the HA-tagged Nanog. We hypothesized that the Nanog doublet consists of; Nanog in the lower band and phospho-Nanog in the upper band. The mutated form of Nanog was no longer being able to be phosphorylated, explaining the accumulation in a lower band form of the Nanog doublet. Addition of MG132 showed an overall increase in protein level in +/-LIF conditions (Fig. 15), this also was consistent with the confocal data showing a retention of Nanog protein even after removal of LIF (Fig.12, 13, 14). However, addition of MG132 resulted in a shift to the upper band form of Nanog in both the wild type and mutant cell lines. This data opposes the hypothesis that the upper band form of Nanog is a GSK3*β* phosphorylated form of Nanog. These results conclude that; the upper band form of the Nanog doublet is not a phosphorylated specifically by GSK3*β*, or that sites mutated in the constructs (GSK3*β* conserved phosphorylation sites) do not play a role in this interaction. To further investigate the importance of the GSK3*β* canonical phosphorylation sites on Nanog, we preformed the same experiment R1 mESCs and the previously used constructed cell lines in the presence and absence of LIF, MG132 and BIO (Fig. 16). We hypothesized that if GSK3*β* is acting through these phosphorylation sites than we would expect to see an effect on the Nanog$^{wt}$HA samples, but not the mutants. In this blot there is an almost complete loss of Nanog protein in cells grown for 3 days in –LIF conditions. The addition of MG132 showed retention of some Nanog protein, and it was mostly located to the upper band form of the Nanog doublet (Fig. 16). The addition of BIO resulted in the retention of Nanog protein, and it was shown to be located mainly in a lower band form for both wt

and mutant cell lines (Fig. 16). This led us to hypothesize that the change in the banding pattern was due to the effects of the proteasome inhibition by MG132, and not on the direct effects of a possible GSK3$\beta$-mediated phosphorylation. To better understand the modifications occurring, immunoprecipitations (IP's) were preformed on R1 and the three tagged cell lines. HA-conjugated beads (sigma) were used to immunoprecipitate HA protein, and the eluate was electrophoresed and probed with: anti-Nanog, anti-HA, anti-phospho-serine, and anti-phospho-threonine antibodies (Fig.17). Western blots were done on whole cell lysates to accompany the IP's. Results showed many non-specific bands, and showed no significant differences in phospho-Nanog between Nanog$^{wt}$HA, Nanog$^{T48A}$HA, and the Nanog$^{T48A/S52A}$HA cell lines.

**5.3 Stability of Nanog-HA Mutant**

We hypothesized that the mutations at the GSK3$\beta$ phosphorylation site of Nanog were somehow stabilizing the Nanog protein and delaying its degradation. To confirm this, a cycloheximide chase experiment was done to compare the rate of Nanog degradation in the Nanog$^{wt}$HA cell line as compared to the rate of Nanog degradation in the Nanog$^{T48A}$HA cell line. Cycloheximide (CHX) is an inhibitor of protein synthesis; therefore its addition to cell cultures and harvesting at subsequent intervals is a useful tool in determining the rate of a particular proteins degradation. Nanog$^{T48A}$HA maintained a higher level of protein over time as compared to the wild type Nanog, meaning that the T48A mutation within Nanog decreased the proteins rate of degradation, therefore, increasing its stability.

## Chapter 6. DISCUSSION AND FUTURE DIRECTIONS

Nanog is a major factor in ESC pluripotency and self renewal, although its importance has been proven there is still relatively little known about this protein. It is a novel transcription factor, having less than 50% homology with any other proteins discovered to date. Having no other proteins to compare it to makes it difficult to elucidate mechanisms involving its regulation and degradation. Although Nanogs presence is very important in maintaining the ES cell state, almost equally important is understanding how it is regulated, and what causes its decrease and eventual loss during differentiation. Understanding such a mechanism would be very important, and a crucial piece to identifying and comprehending key parts of the stem cell puzzle. Surprisingly we observed a rare sighting of Nanog localized to the cytoplasm in a slower differentiating cell line and proposed that nuclear export of Nanog to the cytoplasm could be involved in its eventual degradation. This was a novel observation, and we postulated that we were only able to capture this transient phenomenon because of the slower differentiation rate of the Rb TKO cell line, and normally an ESC colony would be differentiating too quickly and loss of Nanog would be too rapid to be observed. Upon further investigation we found that cytoplasmic Nanog could be found at very low levels in an R1 mESC in the absence of LIF. We also found that by using the proteasome inhibitor, MG132, we were able to see an increase in cytoplasmic Nanog, implying that it was somehow trapped. Along with retaining Nanog protein levels, addition of MG132 also showed a shift to an 'upper band form' in immunoblotting (Fig. 10). We began to postulate that whatever was causing Nanog to be modified and accumulate in the cytoplasm during removal of LIF could be involved in its mechanism for degradation.

Knowing that phosphorylation could be a prerequisite for ubiquitin-mediated degradation, and that Nanog had been shown to be a phospho-protein (Yates and Chambers 2005), we decided to investigate this possibility. We were able to show that Nanog was indeed a phospho-protein, and blocking ubiquitin-mediated degradation increased this phospho-form of Nanog (Fig.11). We hypothesized that Nanog could exist as two forms in ESCs; Nanog, and phospho-Nanog. Phosphorylation has been shown to be a prerequisite for Ub-mediated degradation in many other proteins, including NF-κB, which contains the highest amount of sequence similarity with Nanog protein. Our candidate of choice responsible for phosphorylating Nanog was GSK3*β*. GSK3*β*'s role in ESC biology is not completely understood, but current work in our lab has shown that it is inactive in pluripotent ESCs and moves to the nucleus and becomes active during differentiation (Bechard and Dalton, unpublished data). Also, our lab had been searching for possible targets for GSK3*β*, and Nanog was found to have a canonical GSK3*β* phosphorylation site. Knowing this we investigated this interaction to understand more about this possible relationship.

Upon addition of BIO, a potent GSK3*β* inhibitor, Nanog levels remained high and localized to the nucleus when grown in the absence of LIF (Fig.8), this showed us that inhibition of GSK3*β* decreased or delayed the degradation of Nanog during early differentiation. Not only was the protein level increased, but it was localized strictly to the nucleus, even with MG132 treatment, causing us to hypothesize that the modification responsible for cytoplasmic Nanog could be reliant on active GSK3β. Western blots of day 3 cells grown in the absence of LIF and treated with BIO showed a higher level of Nanog protein than those cells grown with out BIO. Once we had established a link

between Nanog levels and inhibition of BIO, 3 Nanog-HA cell lines were created; a WT, containing the wt Nanog sequence, a single mutant, Nanog$^{T48A}$HA with the serine in the conserved GSK3$\beta$ sequence mutated to an alanine, and a double mutant, Nanog$^{T48A/S52A}$HA, where the serine and threonine in the conserved GSK3$\beta$ sequence were both mutated to alanines. In an Immunoblot he two mutant cell lines showed a higher tagged Nanog protein expression than the wt, however, the banding patterns seemed to be similar (Fig. 16). If GSK3$\beta$ was indeed the kinase responsible for phosphorylating Nanog than we should see a difference in the banding patterns for the mutants and the wt cell lines. IP's were preformed on the same extracts and conditions. The phospho-serine antibody showed a great deal of non-specific bands and no real variation among the samples tested, the phospho-threonine antibody showed and increase in phosphorylation in the –LIF samples, but not significant variation between cell lines.

Nanog phosphorylation by GSK3$\beta$ could not be directly correlated, but, there was an obvious retention of Nanog protein the mutant cell lines. We wanted to quantify the rate at which the mutant Nanog and wt Nanog cell lines were being degraded to see if there was a significant difference. CHX chase experiments were preformed on Nanog$^{wt}$HA and Nanog$^{T48A}$HA cell lines. It was shown that T48A mutation increased the stability of Nanog protein (Fig. 18). Inhibition of GSK3$\beta$ increases the stability of Nanog protein, but it can not be concluded if that is a direct interaction on the Nanog protein itself, or if GSK3$\beta$ inhibition is maintaining pluripotency and stunting spontaneous –LIF induced differentiation.

Future studies investigating the behavior of Nanog in a constitutively inactive and inducible GSK3$\beta$ cell line would be helpful to more fully understand this possible

relationship. Also, it would be interesting to do a 2-D gel and Mass Spectrometry on the upper and lower band forms of the Nanog doublet to verify, and possibly identify the specific modification occurring. If Nanog is indeed phosphorylated and exported to the cytoplasm during differentiation, then creation of a phospho-Nanog antibody would be very useful in visualizing this; both by immunofluorescent labeling and microscopy, or with immunoblots. It would also be interesting to see if any of these Nanog modifications and interactions are involved in differentiation pathways in Human ESCs.

## REFERENCES


Aubert, J., H. Dunstan, et al. (2002). "Functional gene screening in embryonic stem cells implicates Wnt antagonism in neural differentiation." Nat Biotech **20**(12): 1240-1245.

Auernhammer, C. J. and S. Melmed (2000). "Leukemia-Inhibitory Factor--Neuroimmune Modulator of Endocrine Function." Endocr Rev **21**(3): 313-345.

Avilion, A. A., S. K. Nicolis, et al. (2003). "Multipotent cell lineages in early mouse development depend on SOX2 function." Genes Dev. **17**(1): 126-140.

Beddington, R. S. and E. J. Robertson (1989). "An assessment of the developmental potential of embryonic stem cells in the midgestation mouse embryo." Development **105**(4): 733-737.

Bernstein, B. E., T. S. Mikkelsen, et al. (2006). "A Bivalent Chromatin Structure Marks Key Developmental Genes in Embryonic Stem Cells." Cell **125**(2): 315-326.

Boyer, L. A., T. I. Lee, et al. (2005). "Core Transcriptional Regulatory Circuitry in Human Embryonic Stem Cells." Cell **122**(6): 947-956.

Cai, L., Vrana, Schaller (2006). "Glycogen Synthase Kinase 3- and Extracellular Signal-Regulated Kinase-Dependent Phosphorylation of Paxillin Regulates Cytoskeletal Rearrangement." Molecular and Cellular Biology **26**(7): 2857-2868.

Calrone, L., Young, Dobrota, Sergesketter, Ruiz, Skalnik (2005). "Reduced Genomic Cytosine Methylation and Defective Cellular Differentiation in Embryonic Stem Cells Lacking CpG Binding Protein." Mol Cel Biol **25**(12): 4881-4891.

Cantley, L. C. (2002). "The Phosphoinositide 3-Kinase Pathway." Science **296**(5573): 1655-1657.

Capo-chichi, C. D., M. E. Rula, et al. (2005). "Perception of differentiation cues by GATA factors in primitive endoderm lineage determination of mouse embryonic stem cells." Developmental Biology **286**(2): 574-586.

Cartwright, P., C. McLean, et al. (2005). "LIF/STAT3 controls ES cell self-renewal and pluripotency by a Myc-dependent mechanism." Development **132**(5): 885-896.

Chambers I, A. C., J Broadbent, M Robertson, M Lee, M Li, and A Smith (1997). "Structure of the mouse leukaemia inhibitory factor receptor gene: regulated expression of mRNA encoding a soluble receptor isoform from an alternative 5' untranslated region." Biochem J **15**(328): 879-888.

Chambers, I., D. Colby, et al. (2003). "Functional Expression Cloning of Nanog, a Pluripotency Sustaining Factor in Embryonic Stem Cells." Cell **113**(5): 643-655.

Chambers, I. and A. Smith "Self-renewal of teratocarcinoma and embryonic stem cells." Oncogene **23**(43): 7150-7160.

Coucouvanis, E. and G. R. Martin (1995). "Signals for death and survival: A two-step mechanism for cavitation in the vertebrate embryo." Cell **83**(2): 279-287.

Daizo Koinuma, M. S., Akiyoshi Komuro, Kouichiro Goto, Masao Saitoh, Aki Hanyu, Masahito Ebina, Toshihiro Nukiwa, Keiji Miyazawa, Takeshi Imamura, and Kohei Miyazono (2003). "Arkadia amplifies TGF-β superfamily signalling through degradation of Smad7 " European Molecular Biology Organization **22**(24): 6458-6470.

Do, H.-J., H.-Y. Lim, et al. (2007). "An intact homeobox domain is required for complete nuclear localization of human Nanog." Biochemical and Biophysical Research Communications **353**(3): 770-775.

Fenteany, G. and S. L. Schreiber (1996). "Specific inhibition of the chymotrypsin-like activity of the proteasome induces a bipolar morphology in neuroblastoma cells." Chemistry & Biology **3**(11): 905-912.

Gardner, R. (1983). "Origin and differentiation of extraembryonic tissues in the mouse." Int Rev Exp Pathol. **24**: 63-133.

Henrietta Szutorisz, N. D. (2005). "The epigenetic basis for embryonic stem cell pluripotency." BioEssays **27**(12): 1286-1293.

Hideaki Nakajima, P. K. B., Makoto Handa, and James N. Ihle (2001). "Functional interaction of STAT5 and nuclear receptor co-repressor SMRT: implications in negative regulation of STAT5-dependent transcription." European Molecular Biology Organization **20**(23): 6836-6844.

Humphrey, R. K., G. M. Beattie, et al. (2004). "Maintenance of Pluripotency in Human Embryonic Stem Cells Is STAT3 Independent." Stem Cells **22**(4): 522-530.

J T Lee Jr, a. J. A. M. (2002). "The Raf/MEK/ERK signal transduction cascade as a target for chemotherapeutic intervention in leukemia." Leukemia **16**(4): 486-507.

Jackson, K., Gilbert, Chevassut, Forrester, Ansell, Ramsahoye (2004). "Severe Global DNA Hypomethylation Blocks Differentiation and Induces Histone Hyperacetylation in Embryonic Stem Cells." Mol Cel Biol **24**(20): 8862-8871.

Johnson, M. H. and C. A. Ziomek (1981). "Induction of polarity in mouse 8-cell blastomeres: specificity, geometry, and stability." J. Cell Biol. **91**(1): 303-308.

Kielman, M. F., M. Rindapaa, et al. (2002). "Apc modulates embryonic stem-cell differentiation by controlling the dosage of [beta]-catenin signaling." Nat Genet **32**(4): 594-605.

Koinuma, M. S., Akiyoshi Komuro, Kouichiro Goto, Masao Saitoh, Aki Hanyu, Masahito Ebina, Toshihiro Nukiwa, Keiji Miyazawa, Takeshi Imamura, and Kohei Miyazono (2003). "Arkadia amplifies TGF-β superfamily signalling through degradation of Smad7 " European Molecular Biology Organization **22**(24): 6458-6470.

Korenjak, M. and A. Brehm (2005). "E2F-Rb complexes regulating transcription of genes important for differentiation and development." Current Opinion in Genetics & Development **15**(5): 520-527.

Lee, a. J. A. M. (2002). "The Raf/MEK/ERK signal transduction cascade as a target for chemotherapeutic intervention in leukemia." Leukemia **16**(4): 486-507.

Ludmila Jirmanova, M. A., Stéphanie Gobert-Gosse, Suzy Markossian and Pierre Savatier (2002). "Differential contributions of ERK and PI3-kinase to the regulation of cyclin D1 expression and to the control of the G1/S transition in mouse embryonic stem cells." Oncogene **21**(36): 5515-5528.

Lüscher, B. (2001). "Function and regulation of the transcription factors of the Myc/Max/Mad network." Gene **277**(1-2): 1-14.

Mitsui, K., Y. Tokuzawa, et al. (2003). "The Homeoprotein Nanog Is Required for Maintenance of Pluripotency in Mouse Epiblast and ES Cells." Cell **113**(5): 631-642.

Nagy, A., J. Rossant, et al. (1993). "Derivation of Completely Cell Culture-Derived Mice from Early-Passage Embryonic Stem Cells." Proceedings of the National Academy of Sciences **90**(18): 8424-8428.

Nakajima, P. K. B., Makoto Handa, and James N. Ihle (2001). "Functional interaction of STAT5 and nuclear receptor co-repressor SMRT: implications in negative regulation of STAT5-dependent transcription." European Molecular Biology Organization **20**(23): 6836-6844.

Niwa, H. (2007). "How is pluripotency determined and maintained?" Development **134**(4): 635-646.

Niwa, H., T. Burdon, et al. (1998). "Self-renewal of pluripotent embryonic stem cells is mediated via activation of STAT3." Genes Dev. **12**(13): 2048-2060.

Orkin, S. H. (2005). "Chipping away at the Embryonic Stem Cell Network." Cell **122**(6): 828-830.

Paling, N. R. D., H. Wheadon, et al. (2004). "Regulation of Embryonic Stem Cell Self-renewal by Phosphoinositide 3-Kinase-dependent Signaling." J. Biol. Chem. **279**(46): 48063-48070.

Pan, G. J. and D. Q. Pei (2003). "Identification of two distinct transactivation domains in the pluripotency sustaining factor nanog." Cell Res **13**(6): 499-502.

Rasmussen, T. (2003). "Embryonic stem cell differentiation: A chromatin perspective." Reproductive Biology and Endocrinology **1**(1): 100.

Rea, S., F. Eisenhaber, et al. (2000). "Regulation of chromatin structure by site-specific histone H3 methyltransferases." Nature **406**(6796): 593-599.

Reya, T. and H. Clevers (2005). "Wnt signalling in stem cells and cancer." Nature **434**(7035): 843-850.

s. Yamanaka, K. O. (2006). "Intracellular signaling pathways regulating pluripotency of embryonic stem cells." Current Stem Cell Reseach Therapy **1**(1): 103-111.

Sato, N., L. Meijer, et al. (2004). "Maintenance of pluripotency in human and mouse embryonic stem cells through activation of Wnt signaling by a pharmacological GSK-3-specific inhibitor." Nat Med **10**(1): 55-63.

Stead E, W. J., Faast R, Conn S, Coldstone S, Rathjen J, Dhingra U, Rathjen Peter, Walker D, Dalton S (2002). "Pluripotent cell division cycles are driven by ectopic Cdk2, cyclin A/E and E2F activities." Oncogene **21**(54): 8320-8333.

Storm, M. P., H. K. Bone, et al. (2007). "Regulation of Nanog Expression by Phosphoinositide 3-Kinase-dependent Signaling in Murine Embryonic Stem Cells." J. Biol. Chem. **282**(9): 6265-6273.

Szutorisz, N. D. (2005). "The epigenetic basis for embryonic stem cell pluripotency." BioEssays **27**(12): 1286-1293.

T Matsuda, T. N., K Nakao, T Arai, M Katsuki, T Heike, and t Yokota (1999). "STAT3 activation is sufficient to maintain an undifferentiated state of mouse embryonic stem cells." European Molecular Biology Organization **18**(15): 4261-4269.

Wang, Z., T. Ma, et al. (2008). "Aromatic Residues in the C-terminal Domain 2 Are Required for Nanog to Mediate LIF-independent Self-renewal of Mouse Embryonic Stem Cells." J. Biol. Chem. **283**(8): 4480-4489.

Watson, A. J. and G. M. Kidder (1988). "Immunofluorescence assessment of the timing of appearance and cellular distribution of Na/K-ATPase during mouse embryogenesis." Developmental Biology **126**(1): 80-90.

Yamanaka, K. O. (2006). "Intracellular signaling pathways regulating pluripotency of embryonic stem cells." Current Stem Cell Reseach Therapy **1**(1): 103-111.

Yates, A. and I. Chambers (2005). "The homeodomain protein Nanog and pluripotency in mouse embryonic stem cells." Biochem. Soc. Trans. **33**(Pt 6): 1518-1521.

Ying, Y. Q., Xiaoxia: Zhoa, Guang-Quan (2002). "Induction of Primordial Germ Cells from Pluripotent Epiblast." The Scientific World Journal **2**: 801-810.

Yoshida-Koide, U., T. Matsuda, et al. (2004). "Involvement of Ras in extraembryonic endoderm differentiation of embryonic stem cells." Biochemical and Biophysical Research Communications **313**(3): 475-481.

Yoshikawa, Y., T. Fujimori, et al. (1997). "Evidence That Absence ofWnt-3aSignaling Promotes Neuralization Instead of Paraxial Mesoderm Development in the Mouse." Developmental Biology **183**(2): 234-242.

Zhang, Y., R. Cao, et al. (2004). "Mechanism of Polycomb Group Gene Silencing." Cold Spring Harbor Symposia on Quantitative Biology **69**(1): 309-318.

## FIGURE LEGEND

**Figure 1. Early Embryonic Development/ ES Cell Derivation**

Schematic of Early Development and ES Cell Derivation from the Inner Cell Mass of the pre-implanted blastocyst.

**Figure 2. Transcriptional Networks Involved in mESC**

Schematic of many of the important player in Embryonic Stem Cell Regulation and the pathways they contribute to.

**Figure 3. Epigenetic Control of Pluripotency**

Diagram of Epigenetic Regulation in Embryonic Stem Cells

**Figure 4. Nanog Protein Sequence Alignment**

Nanog Protein Sequence Alignment of Human, Rat, Mouse, Chimpanzees, and Dog; also showing the conserved domains.

**Figure 5. Nanog Localization in R1 mESC**

Confocal laser scanning of R1 mouse ESCs grown in the presence and absence of LIF for 2 or 3 days on gelatinized chamber slides. Cells were prepared for Immunoflourescence as described in 2.6.7 and pictures were taken at 20 and 40x.

**Figure 6. Nanog Localization in Rb TKO ES cell line.**

Confocal laser scanning of Rb Triple Knockout mESCs were grown for 3 days on gelatinized chamber slides and prepared for Immunoflourescence as described in 2.6.7 and pictures were taken at 40x.

**Figure 7. Nanog Localization +/- LIF, +/-MG132**

Confocal laser scanning of R1 mouse ESCs grown in the presence and absence of LIF for 2 or 3 days. With and without MG132 at a final concentration of 5$\mu$M added 4 hours before

cells were fixed and prepared for Immunoflourescence as described in 2.6.7 and pictures were taken at 20 and 40x.

**Figure 8. Nanog Localization +/- LIF, +/-BIO**

Confocal laser scanning of R1 mouse ESCs grown in the presence and absence of LIF for 2 or 3 days. With and without BIO at a final concentration of 2 $\mu$M. Cells were prepared for Immunofluorescence as described in 2.6.7 and pictures were taken at 20 and 40x.

**Figure 9. Nanog Localization +/-LIF, +/-MG132, +BIO**

Confocal laser scanning of R1 mouse ESCs grown in the presence and absence of LIF for 2 or 3 days. With and without BIO at a final concentration of 2 $\mu$M; with and without MG132 at a final concentration of 5μM added 4 hours before cells were fixed and prepared for Immunofluorescence as described in 2.6.7 and pictures were taken at 20 and 40x.

**Figure 10. Nanog Protein Modification +/- LIF, +/- MG132 Immunoblot**

R1 mESCs were grown in the presence and absence of LIF; with or without MG132 at a final concentration of 5 $\mu$M, added 4 hours before plates were scraped and cells lysed in cold RIPA buffer. Whole cell lysates (20 $\mu$g total protein per lane) were immunoblotted and probed with anti-Nanog and anti-CDK2 Antibodies.

**Figure 11. Nanog Immunoprecipitation +/- LIF, +/- MG132**

R1 mESCs were grown in the presence and absence of LIF; with or without MG132 at a final concentration of 5 $\mu$M, added 4 hours before plates were scraped and cells lysed in cold RIPA buffer**.** 300 $\mu$g of total protein was added to 50 $\mu$l of pre-blocked, anti-Nanog conjugated, protein A-Sepharose beads (2.5.14) and the immunoprecipitated protein was eluted with 100 $\mu$l of laemmli loading buffer. 20 $\mu$l of eluted protein was loaded, immunoblotted, and probed with anti-phospho-Serine Antibody.

**Figure 12. Nanog Localization in Nanog$^{wt}$HA cell line +/-LIF, +/-MG132**

Confocal laser scanning of Nanog$^{wt}$HA mouse ESCs grown in the presence and absence of LIF for 2 or 3 days. With and without MG132 at a final concentration of 5 $\mu$M added 4 hours before cells were fixed and prepared for Immunofluorescence as described in 2.6.7 and pictures were taken at 20 and 40x.

**Figure 13. Nanog Localization in NANOG$^{T48A}$HA cell line +/-LIF, +/-MG132**

Confocal laser scanning of Nanog$^{T48A}$HA mouse ESCs grown in the presence and absence of LIF for 2 or 3 days. With and without MG132 at a final concentration of 5 $\mu$M added 4 hours before cells were fixed and prepared for Immunofluorescence as described in 2.6.7 and pictures were taken at 20 and 40x.

**Figure 14. Nanog Localization in NANOG$^{T48A/S52A}$HA cell line +/-LIF, +/-MG132**

Confocal laser scanning of Nanog$^{T48A/S52A}$HA mouse ESCs grown in the presence and absence of LIF for 2 or 3 days. With and without MG132 at a final concentration of 5 $\mu$M added 4 hours before cells were fixed and prepared for Immunoflourescence as described in 2.6.7.

**Figure 15. Nanog-HA cell line Modifications +/- LIF, +/- MG132 Immunoblot**

Nanog-HA cell lines were grown in the presence and absence of LIF; with or without MG132 at a final concentration of 5 $\mu$M, added 4 hours before plates were scraped and cells lysed in cold RIPA buffer. Whole cell lysates (20 $\mu$g total protein per lane) were immunoblotted and probed with anti-Nanog, anti-HA and anti-CDK2 Antibodies.

**Figure 16. Modification of NANOG-HA cell lines +/- LIF, +/-MG132, +/-BIO Immunoblot**

Nanog-HA cell lines were passaged for 3 days with and with out LIF and in the presence and absence of MG132 (final concentration of 5 $\mu$M) for 4 hours; and with or without BIO

(2 $\mu$M final concentration), prior to lysis in RIPA buffer. Then 300 $\mu$g of cell lysate was immunoprecipitated using anti-HA conjugated beads. Samples were then subjected to SDS/PAGE and then Western Blotting and probed with Phospho-Serine and Phospho-Threonine antibodies.

**Figure 17. Phosphorylation in NANOG-HA cell lines +/- LIF, +/- MG132, +/-BIO Immunoblot**

Nanog-HA cell lines were grown in the presence and absence of LIF; with and without BIO (final concentration of 2 $\mu$M), with and without MG132 (final concentration of 5 $\mu$M) for 4 hours before harvesting. Then 300 $\mu$g of cell lysate was immunoprecipitated using 50 $\mu$l of anti-HA conjugated beads (Sigma) per sample. Protein was eluted of beads with 100 $\mu$l of laemmli loading buffer, and wells were loaded with 20 $\mu$l, per well. Samples were then subjected to SDS/PAGE and then Western Blotting and probed with Phospho-Serine and Phospho-Threonine antibodies.

**Figure 18. Stability of Nanog vs. NANOG$^{T48A}$HA**

a. Nanog-HA cell lines were grown in LIF for 3 days and treated with cycloheximide (CHX, 10 $\mu$M), and at 30 minute intervals cells were harvested and whole cell lysates prepared. Time points were subjected to Immunoblotting and probed with anti-Nanog Antibody.

b. Graphical representation of decrease in Nanog protein levels. Densitometry was used on Western Blot, using ImageJ 1.40g (Wayne Rasband, NIH, USA). Blue line is NANOG$^{wt}$HA, Pink line is NANOG$^{T48A}$HA.

**FIGURES**

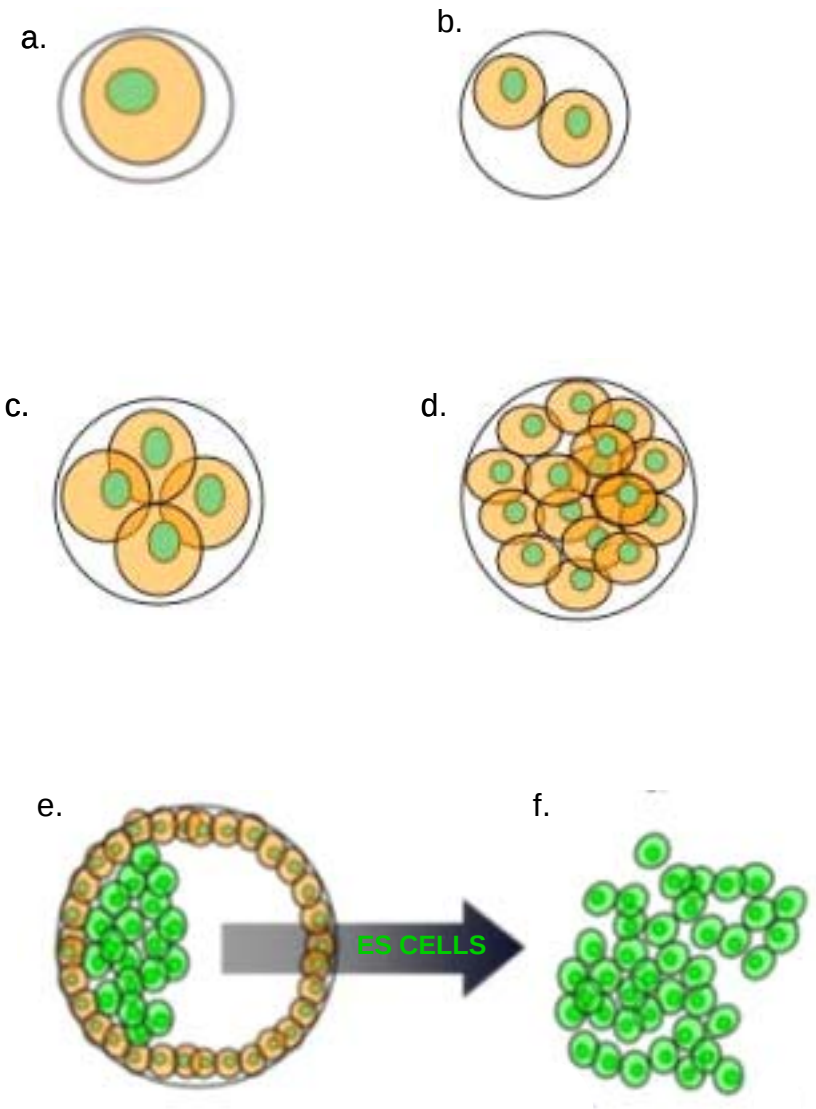


Adapted from Rasmussen et al, 2003

Figure 1: Early Embryonic Development/ ES Cell Derivation

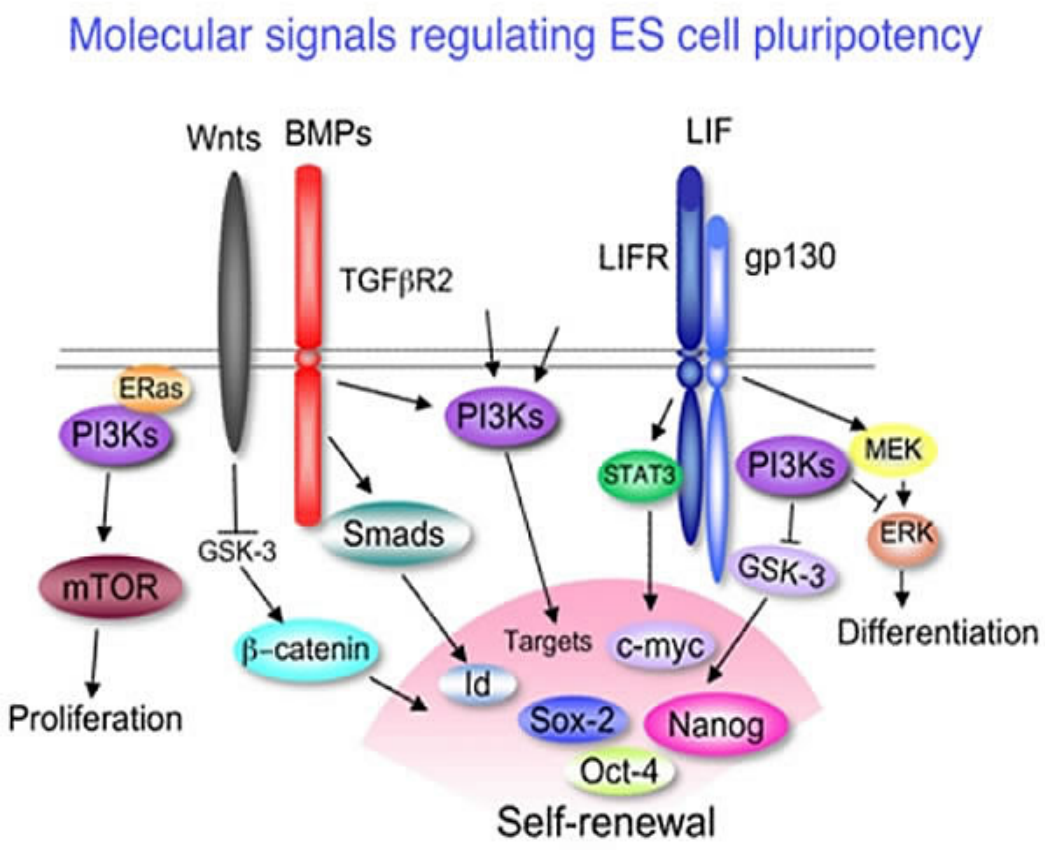


Taken from: M.J.Welham. Department of Pharmacy and Pharmacology, University of Bath 2007

Figure 2: Transcriptional Networks Involved in mESC

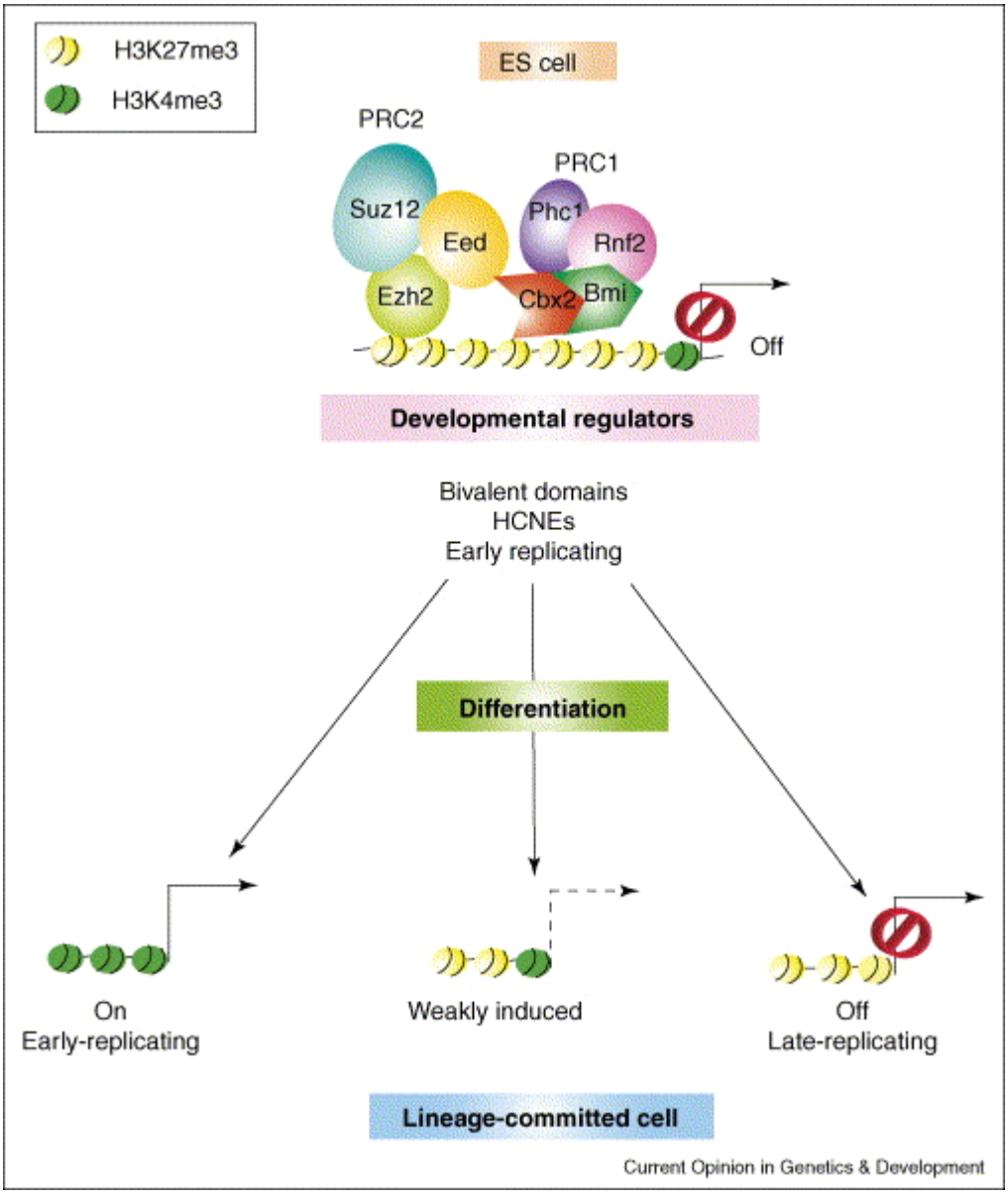


Taken from: Boyer, et al, 2006. **Molecular Control of Pluripotency**

Figure 3: Epigenetic Control of Pluripotency

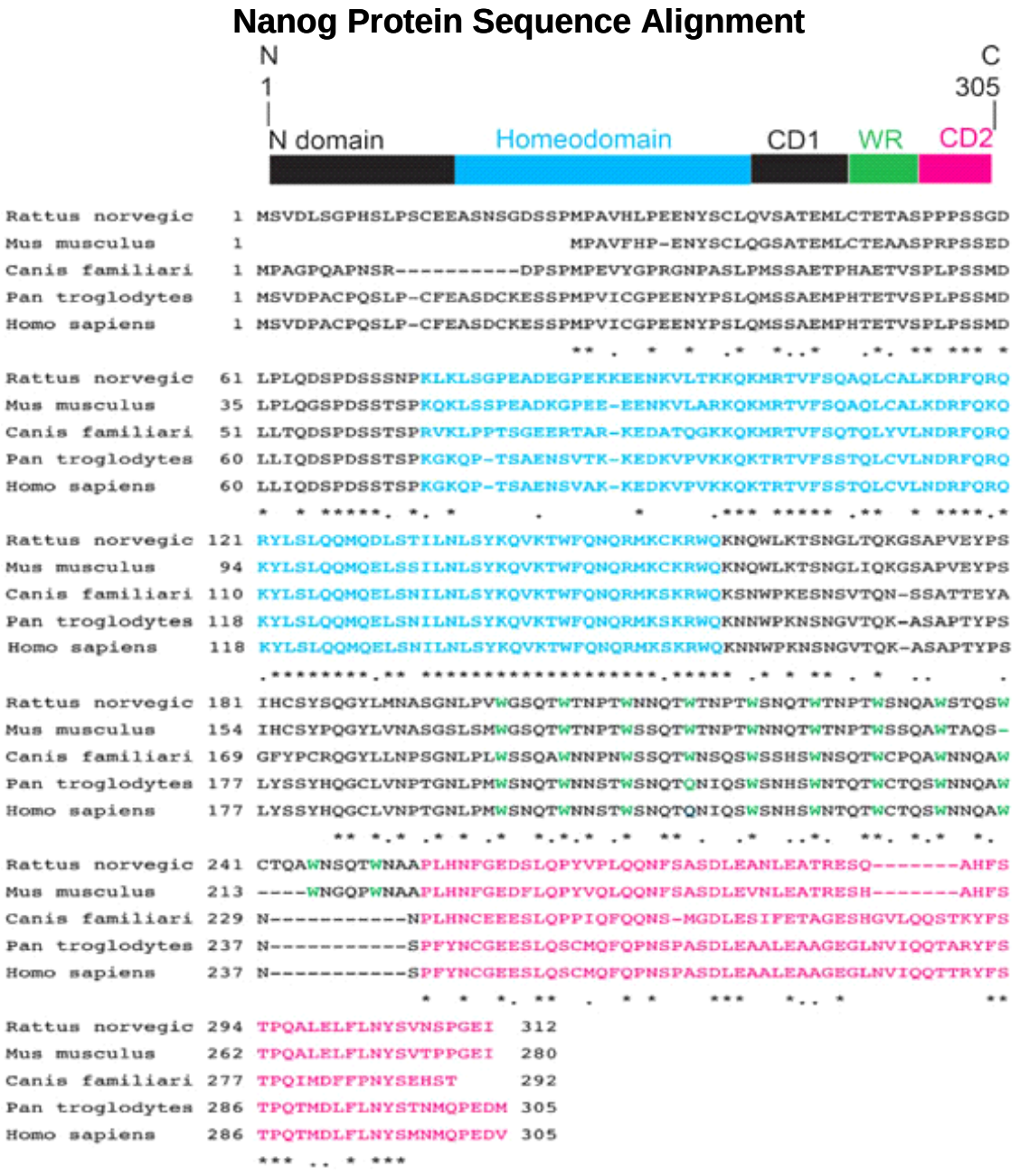


Taken from: **Nanog and transcriptional networks in embryonic stem cell pluripotency**
Guangjin Pan and James AThomson, 2006

Figure 4: Nanog Protein Sequence Alignment

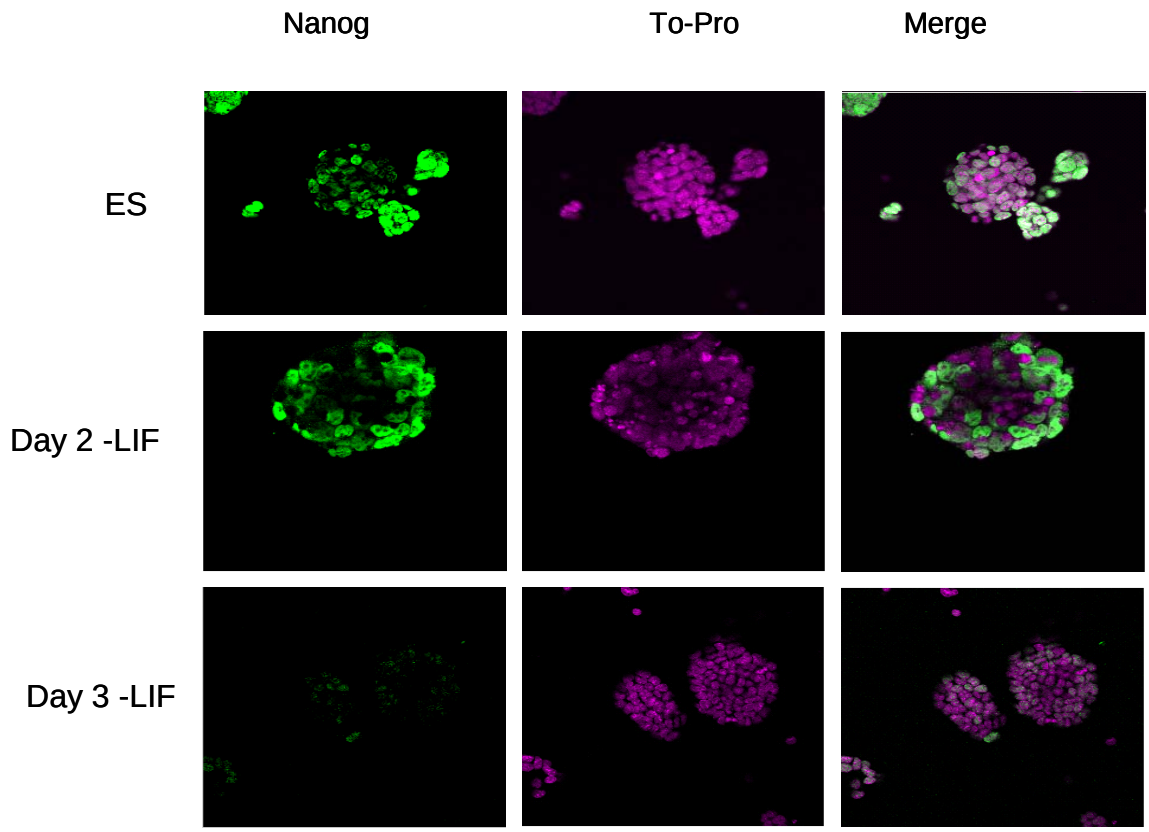


Figure 5: Nanog Localization in R1 mESC

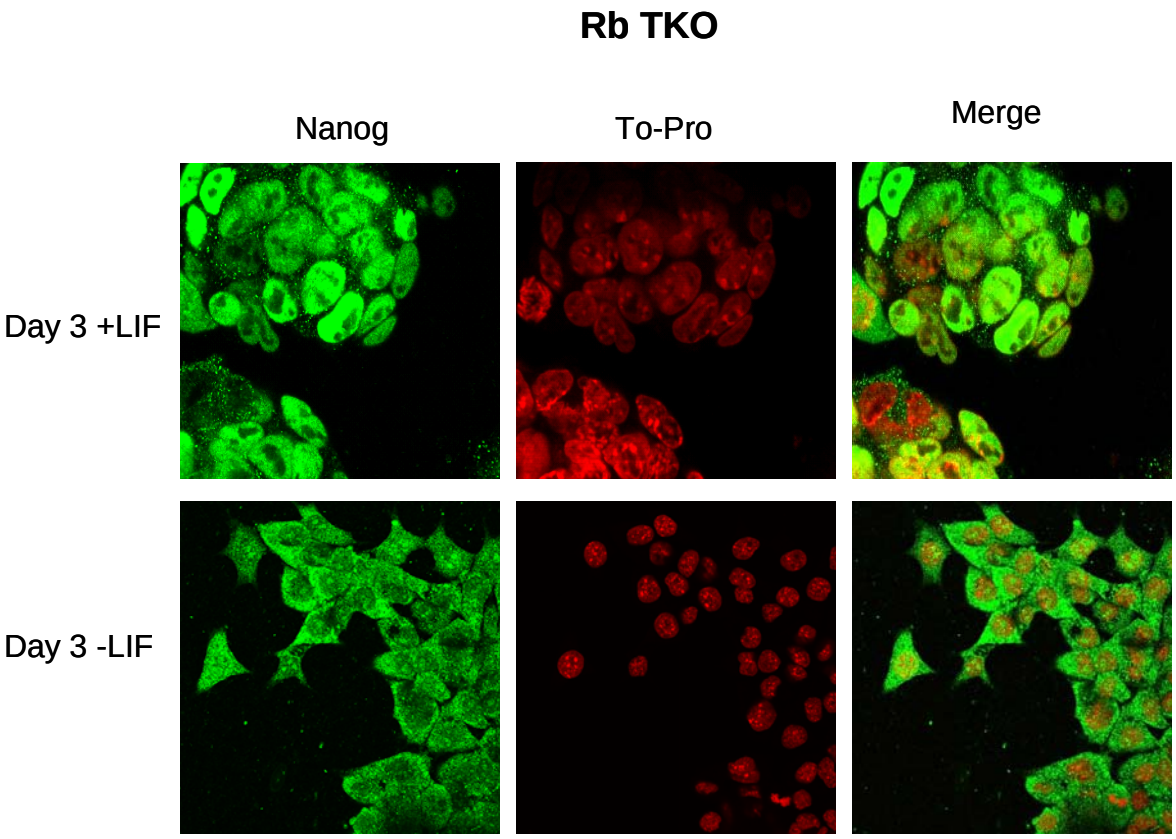


Figure 6: Nanog Localization in Rb TKO ES cell line

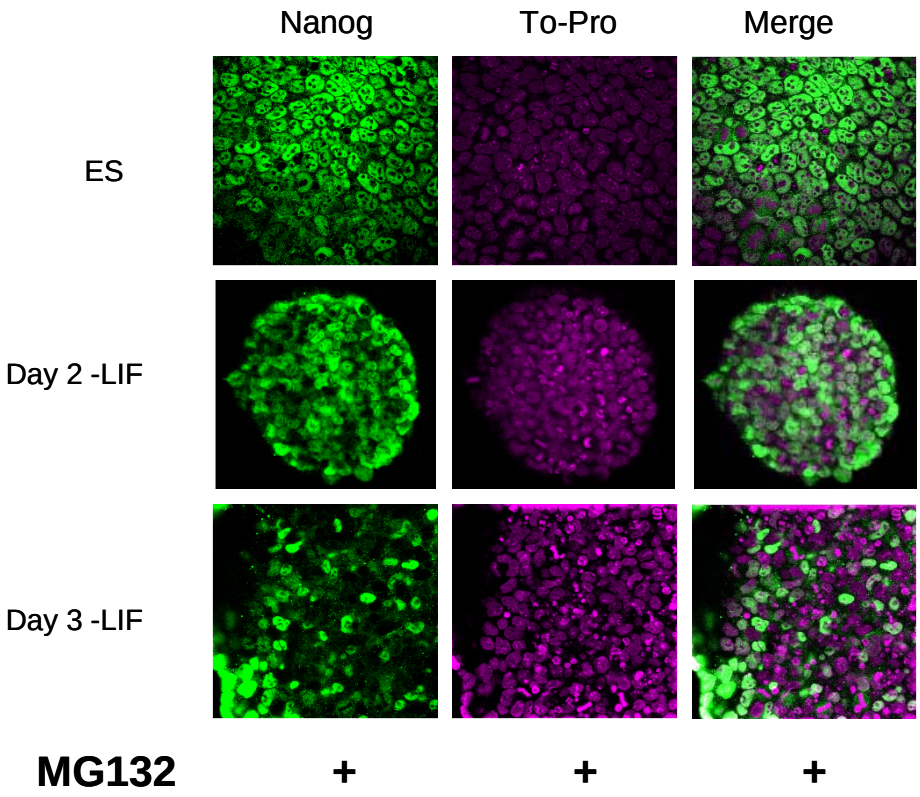


Figure 7: Nanog Localization +/- LIF, + MG132

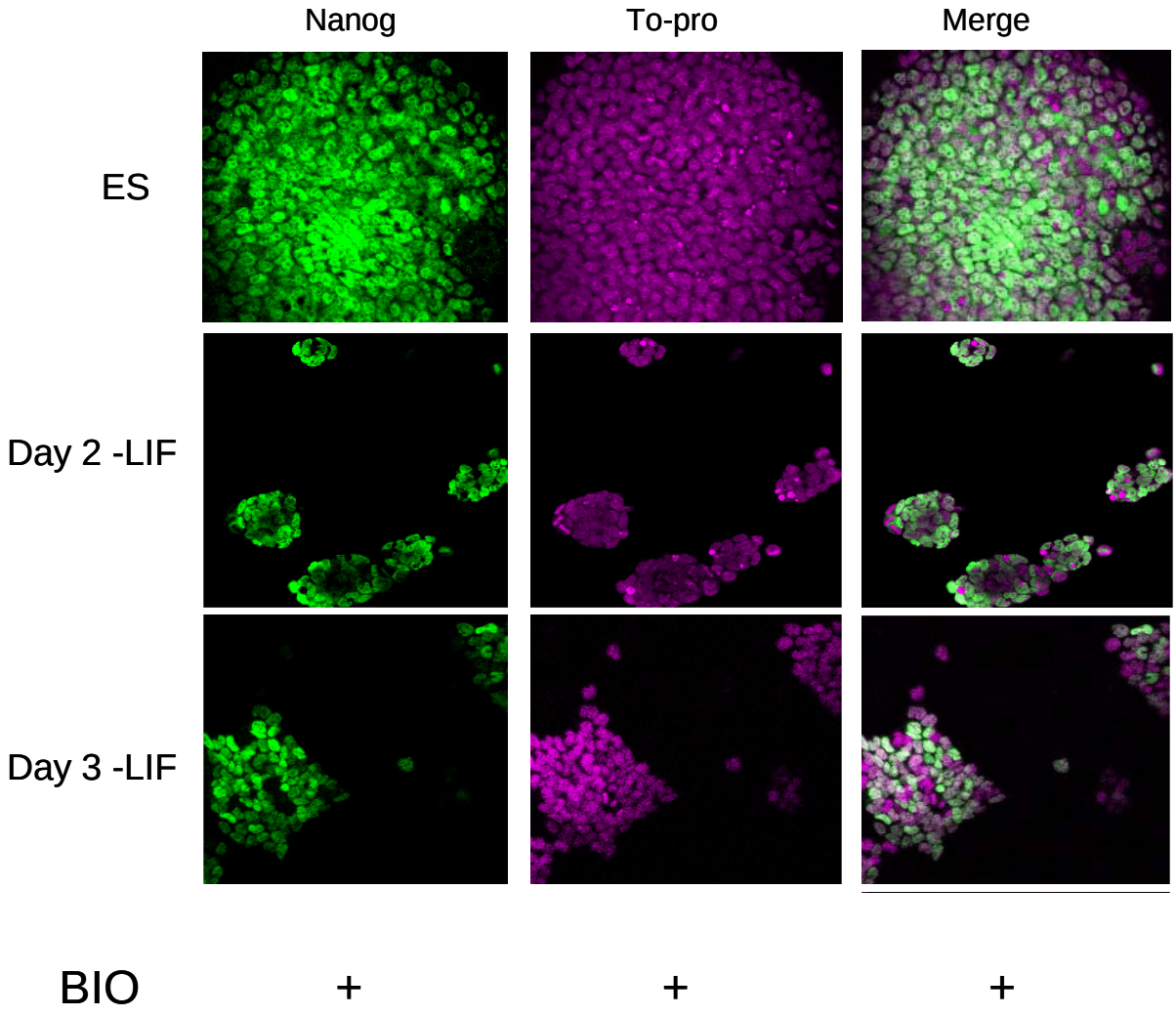


Figure 8: Nanog Localization +/- LIF, +BIO

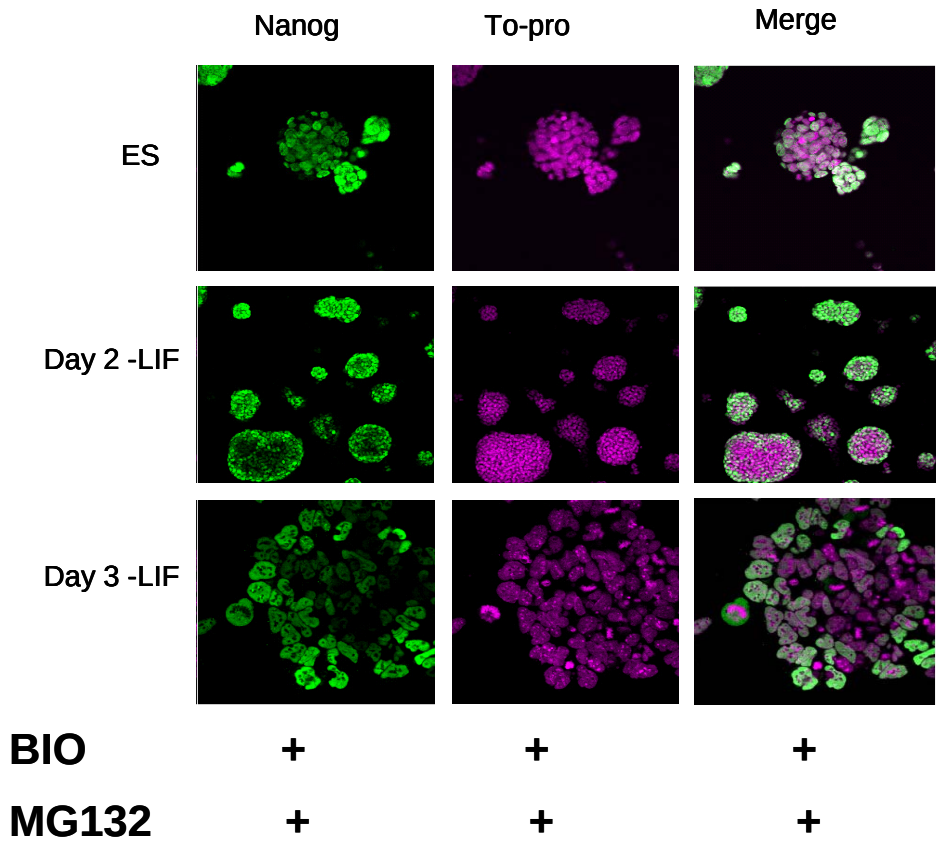


Figure 9: Nanog Localization +/-LIF, +MG132, +BIO

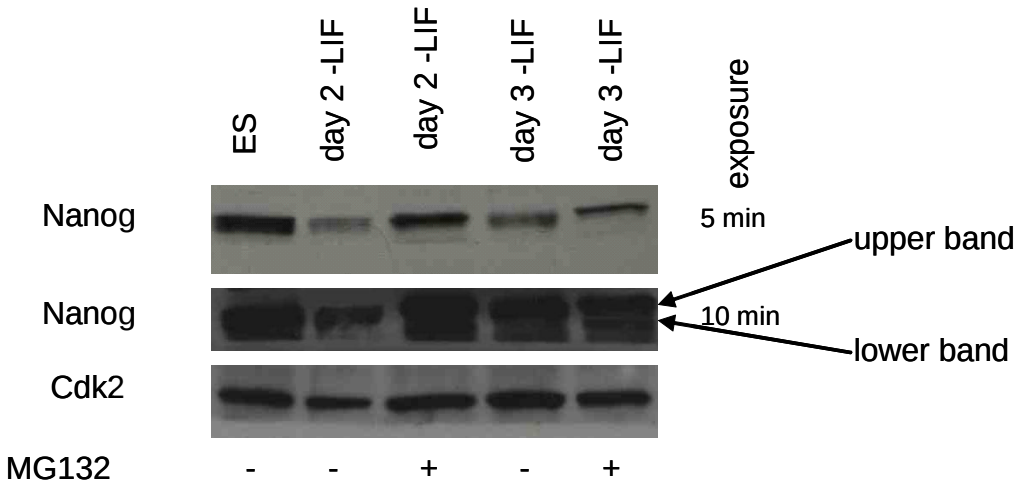


Figure 10: Nanog Protein Modification +/- LIF, +/- MG132 Immunoblot

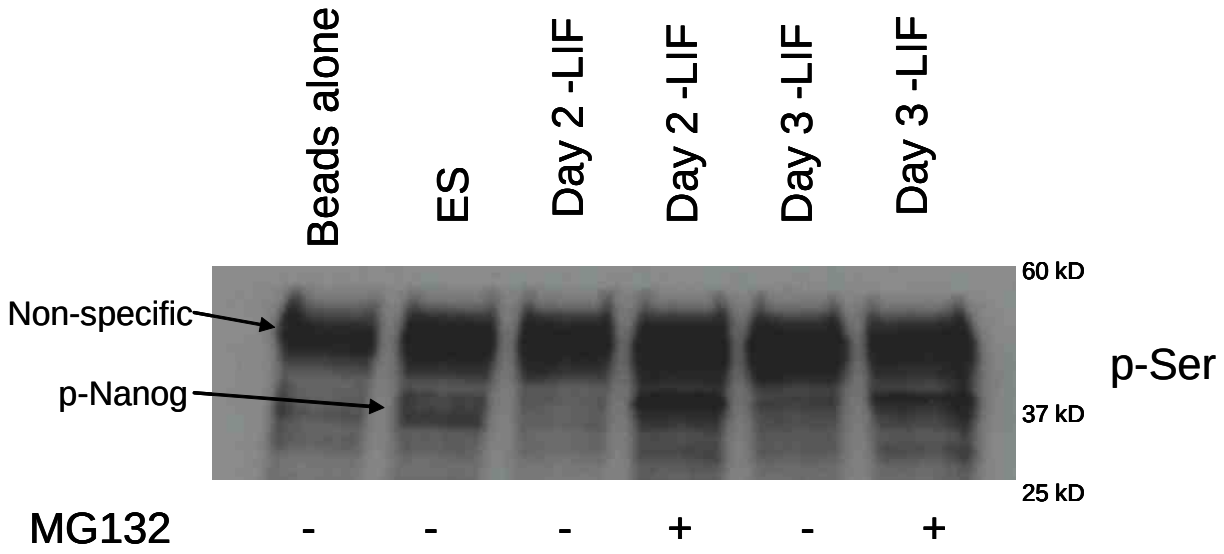


Figure 11: Nanog Immunoprecipitation +/- LIF, +/- MG132

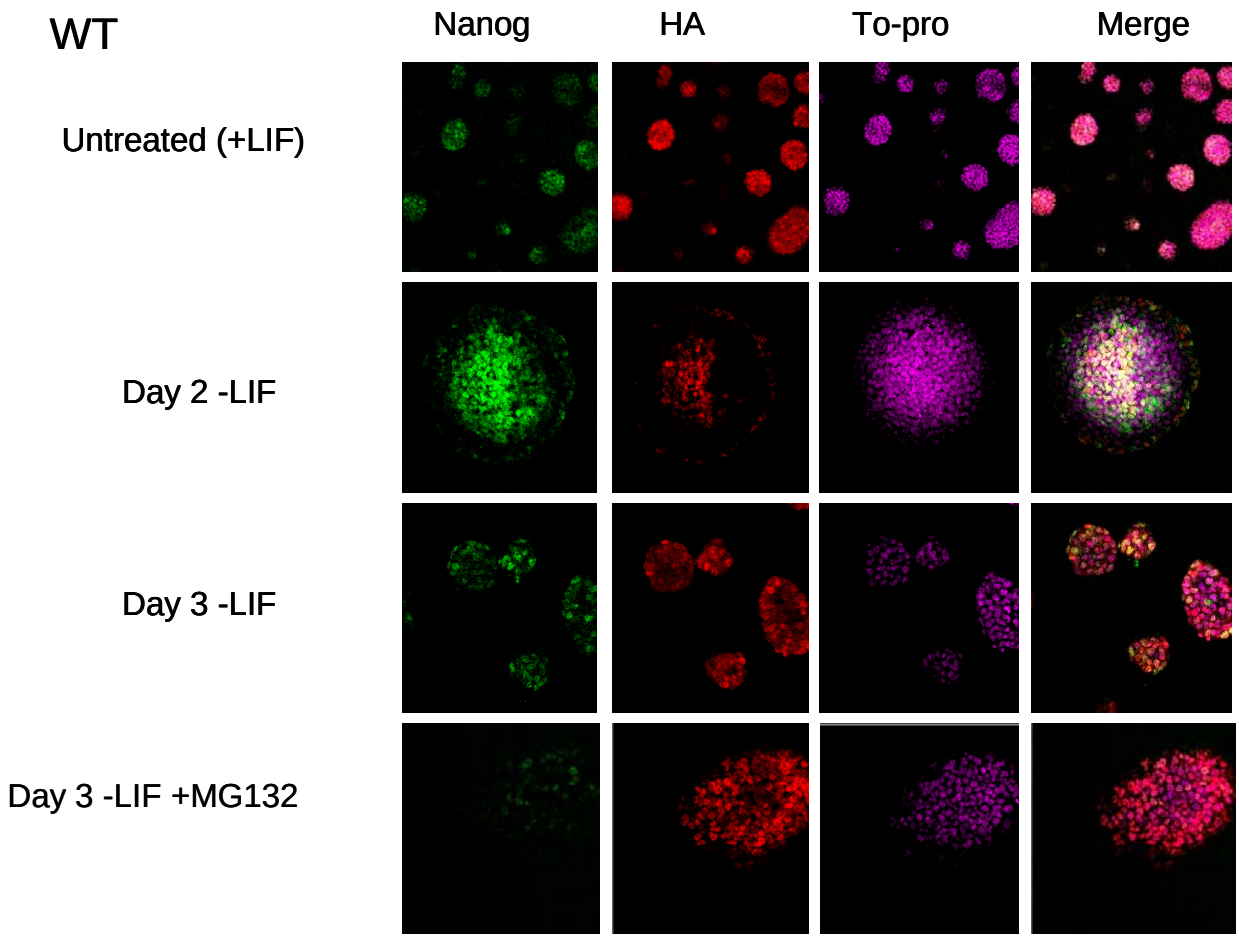


Figure 12: Nanog Localization in NANOG$^{wt}$HA cell line +/-LIF, +/-MG132

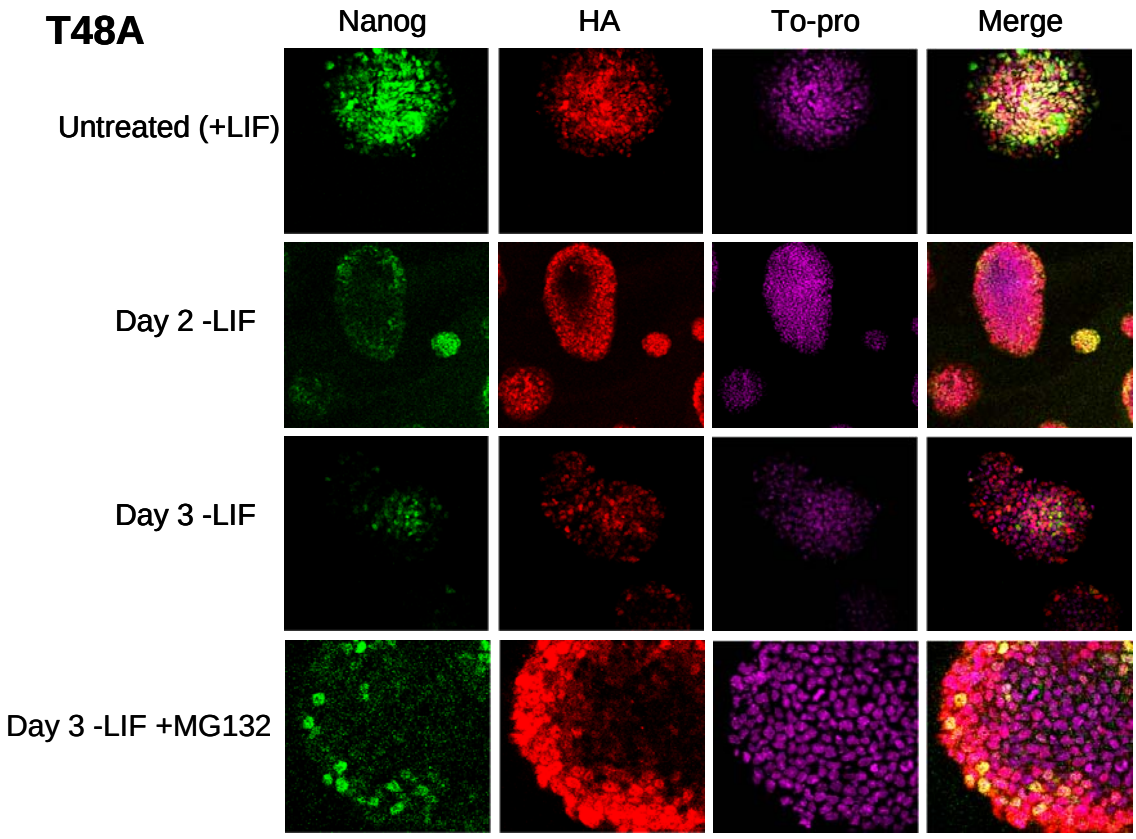


Figure 13: Nanog Localization in NANOG$^{T48A}$HA cell line +/-LIF, +/- MG132

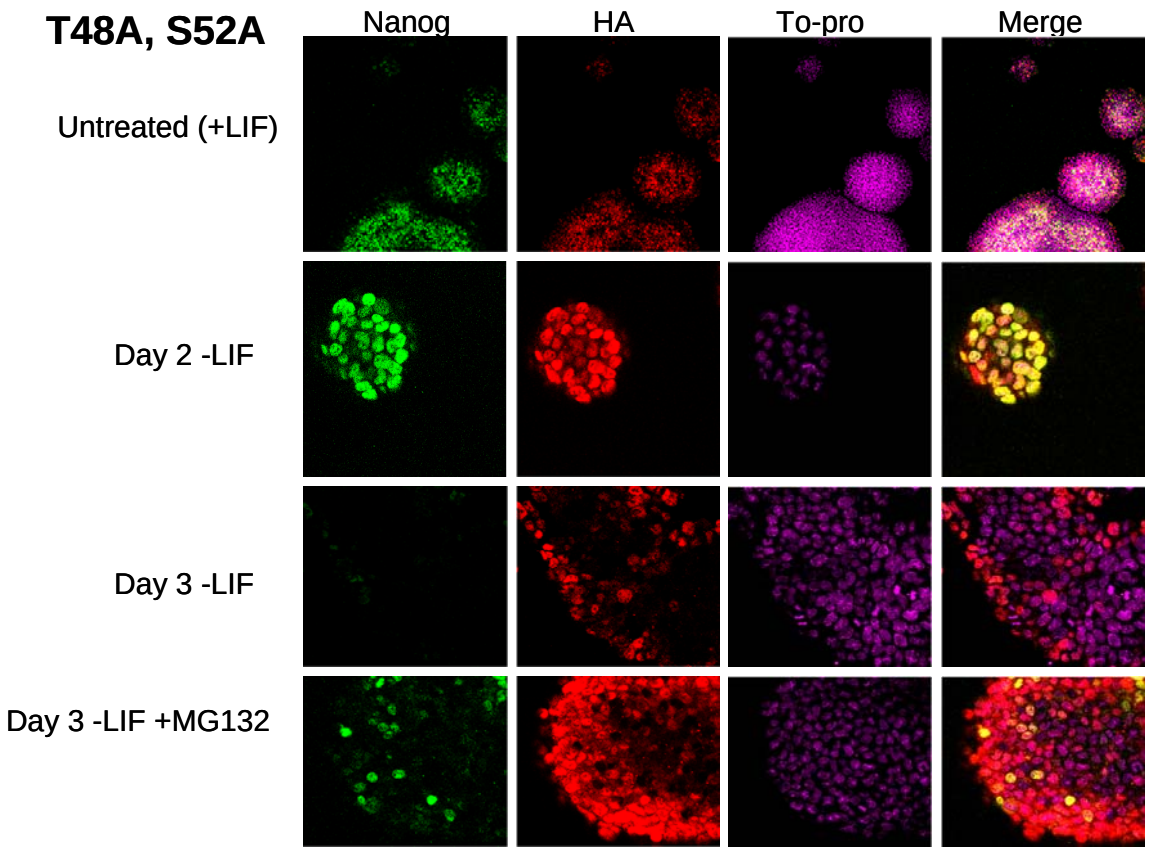


Figure 14: Nanog Localization in NANOG$^{T48A/S52A}$HA cell line +/-LIF, +/- MG132

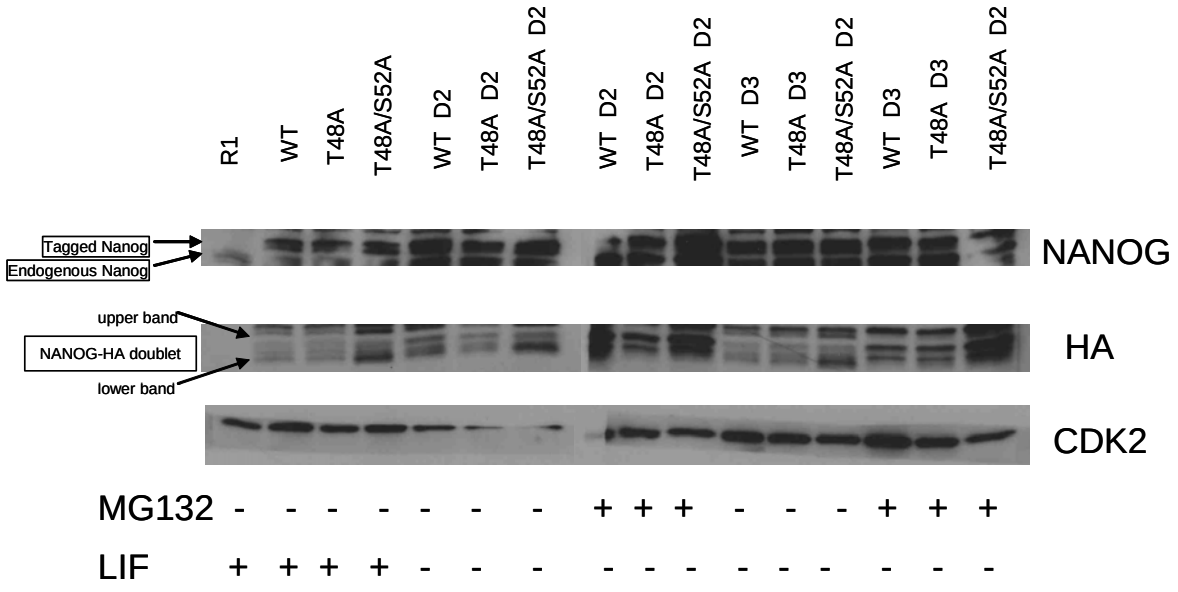


Figure 15: Nanog-HA cell line Modifications +/- LIF +/- MG132 Immunoblot

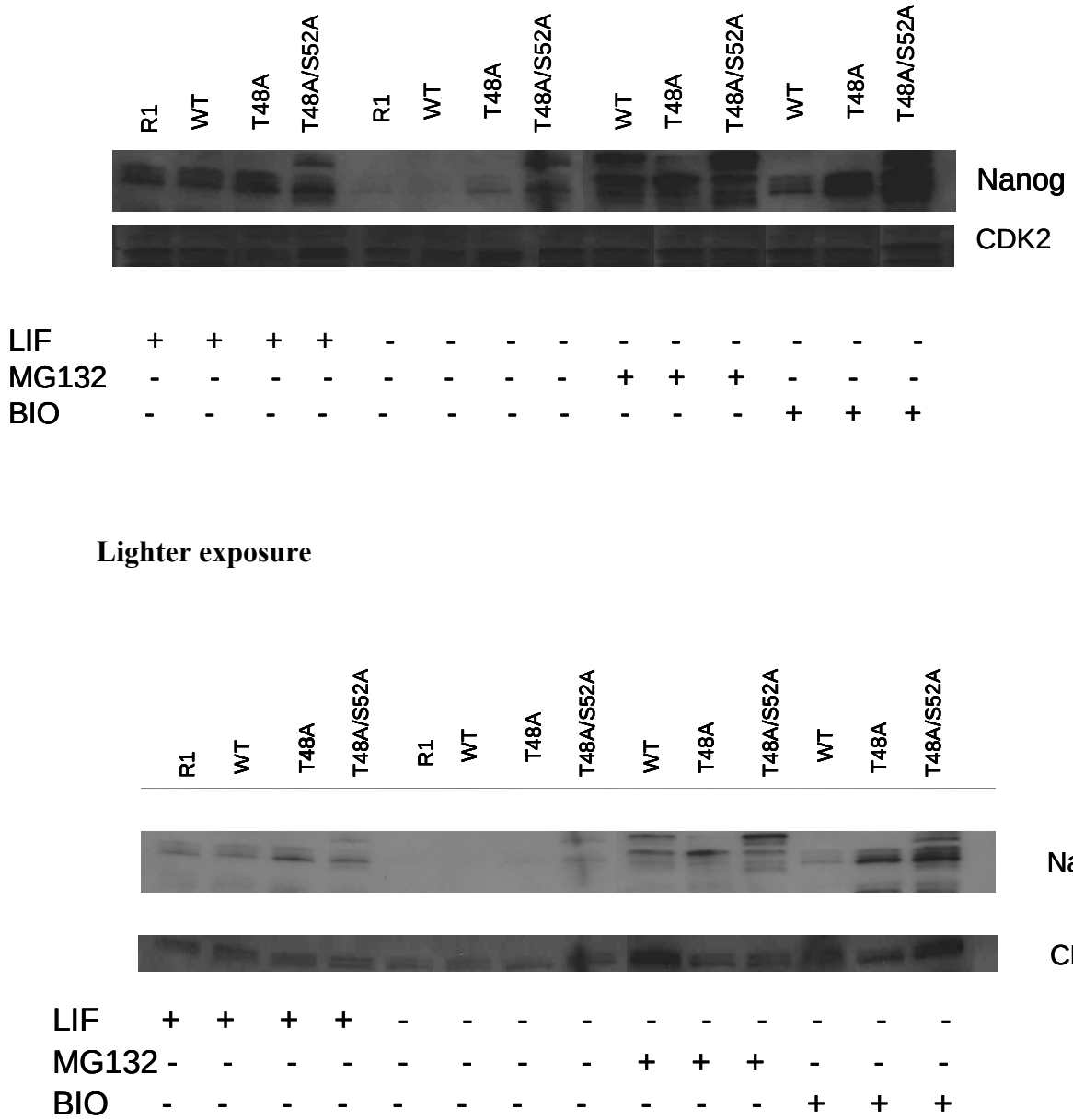


Figure 16: Modification of NANOG-HA cell lines +/- LIF, +/-MG132, +/-BIO Immunoblot

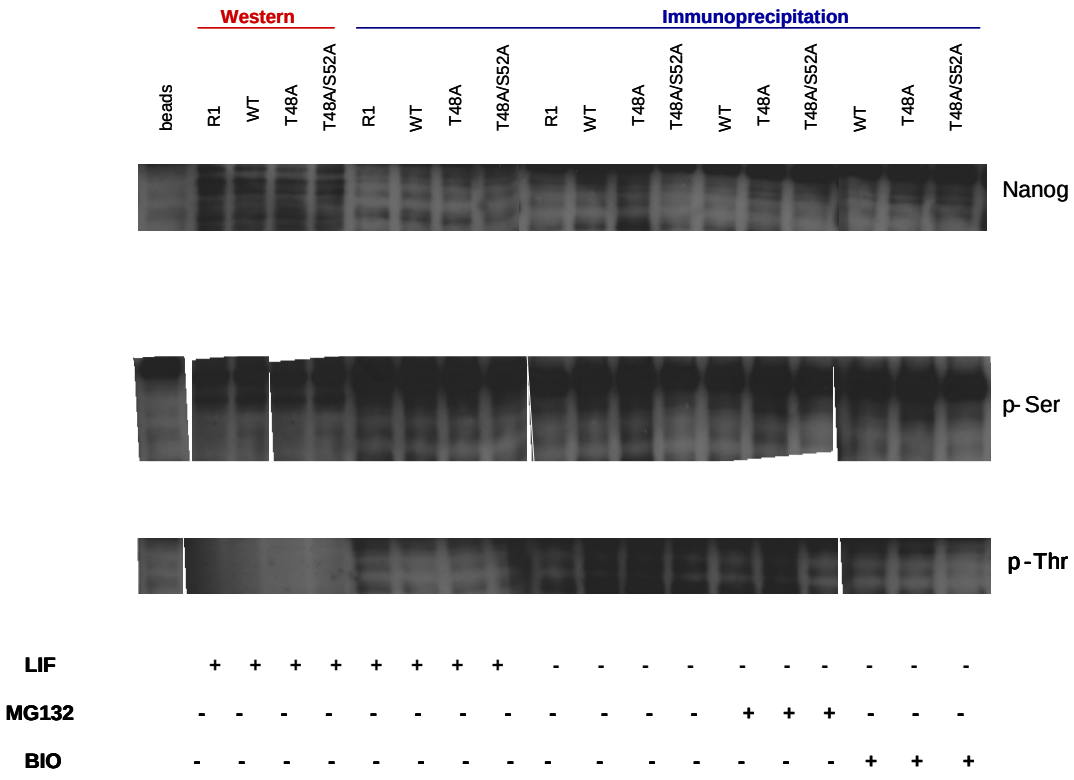


Figure 17: Phosphorylation in NANOG-HA cell lines +/- LIF, +/- MG132, +/-BIO Immunoblot

A.

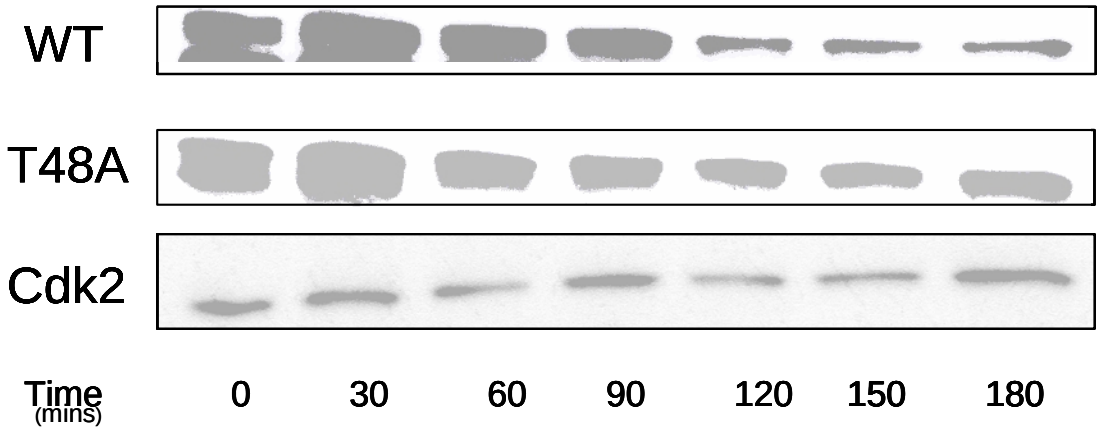


B.

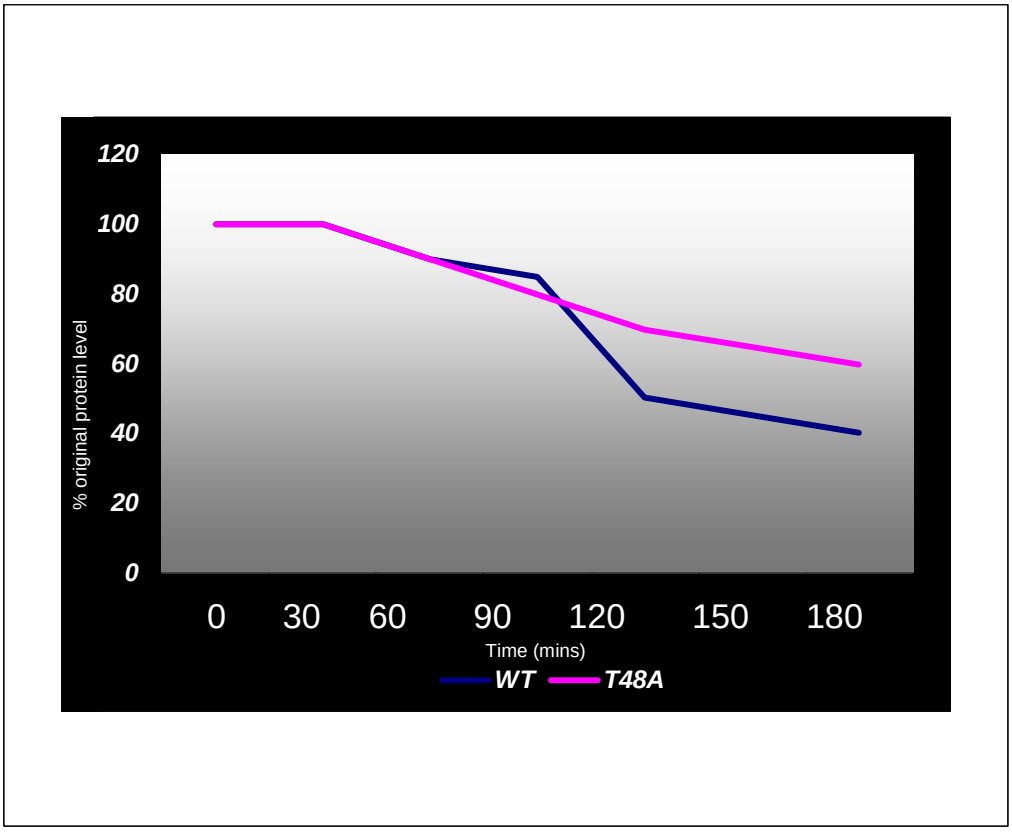


Figure 18: Stability of Nanog$^{WT}$HA vs. NANOG$^{T48A}$HA